



UNIVERSITÀ POLITECNICA DELLE MARCHE

FACOLTÀ DI MEDICINA E CHIRURGIA

PhD Course in Biomedical Sciences

XXXVI cycle

**In silico, in vitro, and in vivo human
metabolism of a new semi-synthetic
cannabinoid: Hexahydrocannabinol
(HHC) and its stereoisomers**

PhD Student:

Dott. Filippo Pirani

Tutor:

Prof. Francesco Paolo Busardò

A.A. 2022/2023

1. ABSTRACT	pag. 3
2. NATURAL, SEMI-SYNTHETIC, AND SYNTHETIC CANNABINOIDS	pag. 5
2.1 Natural cannabinoids	pag. 5
2.2 Semi-synthetic cannabinoids	pag. 10
2.3 Synthetic cannabinoids	pag. 13
2.4 The endocannabinoid system	pag. 17
2.5 Effects of Cannabis, Semi-synthetic, and Synthetic Cannabinoids	pag. 25
2.6 Legislative aspects	pag. 30
3. HEXAHYDROCANNABINOL	pag. 32
3.1 History and diffusion	pag. 32
3.2 Name, Structure, and Chemical Properties	pag. 39
3.3 Synthesis of HHC	pag. 44
4. OBJECTIVES OF THE RESEARCH	pag. 48
5. IN SILICO AND IN VITRO METABOLISM	pag. 49
5.1 Materials and Methods	pag. 49
5.1.1 In silico predictions	pag. 49
5.1.2 Chemicals and reagents	pag. 50
5.1.3 Hepatocyte incubation	pag. 51
5.1.4 Sample preparation	pag. 52
5.1.5 HHC positive urine samples	pag. 42
5.1.6 LC-HRMS/MS settings	pag. 53
5.2 Results	pag. 54
6. DEVELOPMENT AND VALIDATION OF A STEREOSELECTIVE BIOANALYTICAL METHOD IN UHPLC-MS/MS	pag. 59
6.1 Material and Methods	pag. 59
6.1.1 Chemicals and materials	pag. 59
6.1.2 Calibrators and quality control (QC) solutions	pag. 59
6.1.3 HHC on positive samples	pag. 61
6.1.4 Sample preparation	pag. 61
6.1.4.1 Blood and oral fluid	pag. 62
6.1.4.2 Urine	pag. 62

6.1.5 High-performance liquid chromatography tandem mass spectrometry (HPLC-MS/MS) analysis	pag. 63
6.2 Method validation	pag. 65
6.2.1 Linearity	pag. 66
6.2.2 Limit of detection and quantification	pag. 66
6.2.3 Carryover and Interferences	pag. 67
6.2.4 Dilution integrity and stability	pag. 68
6.2.5 Matrix effect and recovery	pag. 70
6.3 Results	pag. 71
6.3.1 Method development	pag. 71
6.3.2 Method validation	pag. 75
6.4 Application to human samples	pag. 79
7. IN VIVO METABOLISM	pag. 82
7.1 Methods	pag. 82
7.2 Data Analysis and Results	pag. 84
7.3 Clinical evidence of in vivo administration of HHC	pag. 96
8. DISCUSSION	pag. 103
9. CONCLUSIONS	pag. 117
10. BIBLIOGRAPHY	pag. 119

1. ABSTRACT

Since 2021, there was an overall increase in reports of herbal material where natural cannabinoids were found alongside synthetic cannabinoids in at least 13 European countries. It results in a growing concern that consumers of cannabis may be at risk of inadvertent exposure to synthetic cannabinoids. New regulatory challenges have emerged about the commercialization of cannabis derivatives and about the recreational drug market. In 2022, the appearance of new semi-synthetic cannabinoids reflected these concerns. Hexahydrocannabinol (HHC) was identified in May 2022 and had been reported by 20 EU Member States by March 2023. The effects of HHC in humans have not been studied, but consumers and reports suggest they may be subjectively similar to those of cannabis. Some of the products are available in forms that may deliver high doses, raising concerns about the possible implications for public health. The purpose of this thesis was to identify the main metabolites of HHC through *in silico* and *in vitro* studies in order to identify biomarkers of consumption. Subsequently, a method using Ultra-high performance liquid chromatography tandem mass spectrometry (UHPLC-MS/MS) was developed and fully validated for their detection in biological matrices. Finally,

the identification and quantification of HHC stereoisomers and metabolites were carried out on real samples of oral fluid, blood, and urine from individuals who had smoked a known quantity of HHC.

2. NATURAL, SEMI-SYNTHETIC, AND SYNTHETIC CANNABINOIDS

2.1 Natural cannabinoids

Natural cannabinoids are the primary constituents of the Cannabis plant and are not found anywhere else in nature. In the Cannabis plant, over 500 components have been identified, with more than 100 classified as “cannabinoids” due to their chemical structure. These molecules share the ability to interact with cannabinoid receptors in our body [1].

Cannabis is one of the most well-known and historically utilized psychoactive plants. Throughout antiquity, its fibers were used for textile and cord production, its seeds for oil and fuel production, and its active compounds for medical, religious, and recreational purposes, especially in Asian regions and Northern Europe [2] [3].

However, therapeutic use gained popularity in Europe and America only in the 19th century. Preparations and tinctures based on Cannabis were used for the treatment of neurological and autoimmune conditions such as seizures, migraines, rheumatism, malaria, and gout. Despite this, due to the rapid and increasing

popularity of recreational cannabis use, it was soon recognized as an illegal substance, due to its adverse effects and potential for abuse [4].

Despite this prohibition, to date, it continues to be the most consumed drug worldwide and therefore remains one of the most studied and closely monitored substances from a chemical-toxicological perspective. In fact, according to data reported by the United Nations Office on Drugs and Crime (UNODC), approximately 4% of the global population between the ages of 15 and 64 (209 million people) have used cannabis at least once. These figures have increased by nearly 18% in the last 10 years and continue to grow, especially in North America (Canada and the USA), Central Europe, and Eastern Europe. Compared to adults, higher consumption has been reported among teenagers in the last year (5.8% in the age group 15-16 years) [5].

Phytocannabinoids, compounds naturally present in and derived from the Cannabis plant, are divided into 10 subclasses: cannabigerols, cannabichromenes, cannabidiols, Δ^8 -tetrahydrocannabinols, Δ^9 -tetrahydrocannabinols, cannabicyclols, cannabielsoins, cannabinols, cannabinodiols, and cannabitriols [6]. They are biosynthesized and accumulated as cannabinoid acids and then undergo

decarboxylation, resulting in the formation of their biologically active form at the receptor level [7].

Specifically, decarboxylation of the precursors yields delta9-tetrahydrocannabinol (Δ^9 -THC) and its metabolite cannabinol (CBN), cannabidiol (CBD), cannabichromene (CBC), and its chemical artifact cannabicyclol (CBL). From geranyl diphosphate and divarinic acid, cannabigerovarinic acid (CBGVA), a C3-phytocannabinoid with a n-propyl side chain, is formed. From CBGVA, the respective cannabinoids are synthesized: Δ^9 -tetrahydrocannabivarinic acid (Δ^9 -THCVA), cannabivarinic acid (CBDVA), and cannabichromevarinic acid (CBCVA). Their decarboxylation forms the respective cannabinoids: Δ^9 -tetrahydrocannabivarin (Δ^9 -THCV), cannabivarin (CBNV), cannabidivarin (CBDV), cannabichromevarin (CBCV), and cannabicyclovarin (CBLV) [8].

Among the various constituents of Cannabis, the aforementioned cannabidiol (CBD) and Δ^9 -tetrahydrocannabinol (Δ^9 -THC or THC) are the most abundant and of broader interest natural cannabinoids. The molecule receiving the most attention and study is Δ^9 -THC, as it is primarily responsible for the psychoactive effects of

Cannabis, while CBD is the second phytocannabinoid present in Cannabis but does not induce the psychoactive effects of THC [9].

Δ^9 -THC (Fig. 1), belonging to the class of tetrahydrocannabinols, is pharmacologically a partial agonist of cannabinoid receptors. Its psychoactive effects, generally acute, transient, and self-limiting, include euphoria, relaxation, altered perception, increased appetite, and analgesia, but also anxiety, paranoia, motor slowing, hypothermia, and catalepsy. These effects are determined by presynaptic inhibition of the release of various neurotransmitters, particularly dopamine, N-methyl-D-aspartate, and glutamate [10].

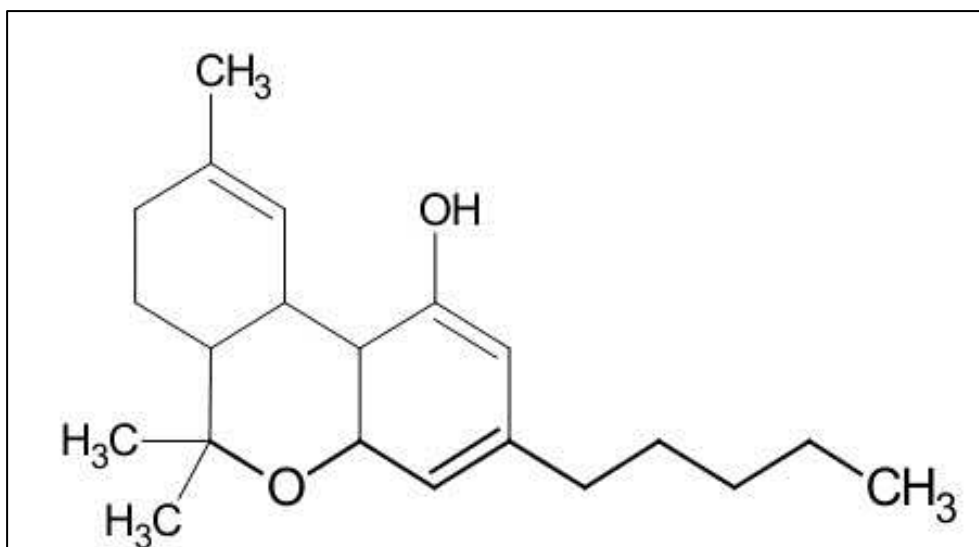


Fig. 1 Chemical structure of Δ^9 -tetrahydrocannabinol

CBD (Fig. 2), belonging to the class of cannabidiols, differs from THC in the presence of a hydroxyl group at position C7, resulting in the loss of the benzene ring structure. Despite structural similarity, it has a lower agonism toward cannabinoid receptors and is considered a negative allosteric modulator [11]. CBD has shown anticonvulsant, antispasmodic, antidystonic, anxiolytic, antiemetic, antiepileptic, neuroprotective, and anti-rheumatoid arthritis properties. Additionally, CBD reduces the side effects of THC on heart rate, respiration, and body temperature while enhancing its analgesic efficacy by prolonging its duration of action [12, 13]. Recently, it has been demonstrated that CBD can act as an inverse agonist of some G protein-coupled receptors (GPR3, GPR6, and GPR12), and based on this interaction, its potential use in Alzheimer's disease, Parkinson's disease, certain types of cancers, and some cases of infertility is being studied [14].

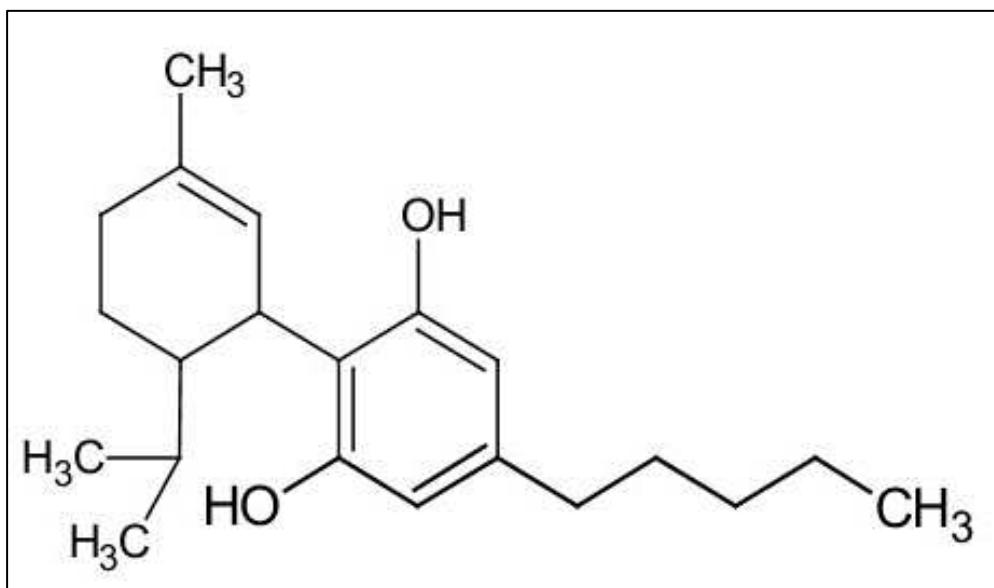


Fig. 2 Chemical structure of cannabidiol (CBD)

2.2 Semi-synthetic cannabinoids

Semi-synthetic cannabinoids (SSCs) refer to molecules that, through chemical manufacturing, derive from natural cannabinoids. The main difference between synthetic cannabinoids (SCs) and semi-synthetics is that the latter retain the structure of natural cannabinoids, with minor chemical modifications aimed at enhancing or refining their pharmacological profile.

In detail, the variation in the chemical structure compared to natural cannabinoids involves certain chemical groups (also called "residues"), whose

modification influences the pharmacological profile. These molecules have not been fully identified, described, or regulated.

An emerging semi-synthetic cannabinoid, structurally related to THC, is hexahydrocannabinol (HHC). Two of its derivatives, HHC-acetate (HHCO) and hexahydrocannabinofuranol (HHCP), are also known [15].

HHC is found in very low doses in the Cannabis plant, and almost all commercially available HHC is obtained semi-synthetically through chemical hydrogenation processes in the laboratory. It has a chemical and molecular structure similar to THC but remains a cannabinoid with different characteristics, which will be further described as the subject of this study.

HHC appears to be a more stable compound than THC and less susceptible to degradation from exposure to heat and light. This characteristic makes it interesting for cannabinoid producers as it allows for long-term preservation. It induces psychoactive effects, similar to THC, and seems capable of binding to cannabinoid receptors of the endocannabinoid system (ECS) in humans [15].

HHC is the first semi-synthetic cannabinoid reported in the EU and monitored as a new psychoactive substance (NPS) by the European Early Warning System

(EWS) since October 21, 2022, but currently, its trade is still legal in many countries worldwide [16].

For a more extensive discussion on HHC, please refer to the following paragraphs.

2.3 Synthetic cannabinoids

In the 1990s, with the discovery of cannabinoid receptors and the subsequent identification of the endogenous ligand, anandamide, research on the possible mechanism of action of cannabinoids, both exogenous and endogenous, experienced acceleration.

The initial goal of the research was to design and synthesize molecules that retained the potentially therapeutic properties of natural cannabinoids while eliminating their typical undesired effects, including those related to the development of dependence. Concurrently, products with other purposes spread, generally synthesized in clandestine laboratories and sold for recreational use [17].

Synthetic cannabinoids are a class of molecules designed in the laboratory to obtain compounds capable of selectively and with varying affinity activating endogenous cannabinoid receptors. Unlike SSCs, they are not structurally related to

natural cannabinoids and are solely produced through chemical synthesis. Initial synthesis attempts were oriented toward molecules entirely analogous to THC; subsequently, there was an evolution in their structural characteristics aimed at identifying binding sites with receptors and consequently producing only the active portions of the molecule, deviating from the classic benzopyranic tricyclic structure of THC.

Because the molecular structures of synthetic cannabinoids differ from THC, their initial use was not prohibited. In the early 2000s, synthetic cannabinoids began being used recreationally in an attempt to achieve effects similar to Cannabis. They quickly gained popularity as they were inexpensive and generally not detectable by standard drug tests.

In 2008, several synthetic cannabinoids were classified as illicit substances; however, new similar compounds are continuously synthesized [18]. In recent years, over 250 illicitly manufactured compounds have targeted the ECS and have been designed to bypass existing regulations on controlled substances [19]. These compounds are generally known as "Spice" (Spice Silver, Spice Gold, Spice

Diamond, Yucatan Fire, Sence, Chill X, Smoke, Genie, Algerian Blend, and many others) or "K2," "Black Mamba," "Scooby Snax," etc. [20, 21].

According to the European Monitoring Centre for Drugs and Drug Addiction (EMCDDA), synthetic cannabinoids are classified into seven main structural groups: naphthoylindoles (e.g., JWH-018, JWH-073, and JWH-398), naphthylmethylindoles, naphthoylpyrroles, naphthylmethyleneindenes, phenylacetylindoles (i.e., benzoylindoles, e.g., JWH-250), cyclohexylphenols (e.g., CP 47.497 and homologues of CP 47.497), and classic cannabinoids (e.g., HU-210).

Among synthetic cannabinoids, by the end of 2008, when the phenomenon exploded in Europe and worldwide, the most commonly found compounds in various herbal blends, also called "herbal mixture" or "herbal blend," were JWH-018 and JWH-073. Subsequently, numerous other synthetic cannabinoids were introduced to the market, such as JWH-200, JWH-250, JWH-122, 5F-THJ, 5F-THJ-018, THJ-018, A-796,260, A834,735, CUMYL-BICA, CUMYL-PINACA, RCS-3, trans-CP 47,497-C8, LS91297, 5-CI-MN-24, 5F-APINACA, 5F-AB-144, 5F-ABICA, 5F-NPB-22, 5FADBICA, 5F-SDB-006, 5F-ADB, FUBINIMA, AM-

678 [22]. The pharmacotoxicological properties of synthetic cannabinoids are not well-known to date, as few studies have been conducted and published on humans. Some cannabinoids may have particularly long half-lives, leading to prolonged psychoactive effects. Additionally, there could be significant variability between and within batches of smoking blends, both in terms of the molecules present and their quantities, increasing the risk of intoxication compared to cannabis.

In Europe, synthetic cannabinoids are monitored as new psychoactive substances by the EWS and constitute the largest group of substances monitored by the EMCDDA. Despite efforts to reduce the availability of synthetic cannabinoids in the drug market, data presented by the EMCDDA through the EWS show their widespread presence in Europe, attributable to various factors, including relatively low cost, easy availability, and high pharmacotoxicological potential. Furthermore, products known to the scientific community quickly become outdated, as the online market is rapidly evolving, and synthetic cannabinoids used in preparations are continually replaced by “legal” alternatives in response to new control measures. They are generally packaged in sachets labeled “not for human consumption” and

often misleadingly advertised as incense, meditation potpourri, or room deodorizers [20, 22].

2.4 The endocannabinoid system

The study of the mechanisms underlying the effects associated with the action of phytocannabinoids has led to the discovery of a complex biological communication system known today as the ECS. However, in the scientific community, the ECS has also been the subject of numerous studies aimed at developing new compounds for potentially therapeutic purposes in a wide variety of disorders.

The ECS is a widespread neuromodulatory network involved in the development of the central nervous system (CNS) and various physiological processes [23]. It consists of cannabinoid receptors (CB1 and CB2), their corresponding endogenous ligands (endocannabinoids), anandamide (AEA), and 2-arachidonoylglycerol (2-AG), as well as enzymes responsible for their biosynthesis, degradation, and transport.

Most components of the ECS are multifunctional; therefore, rather than being a discrete and isolated system, the ECS influences and is influenced by many other

signaling pathways [24]. This neuromodulatory system is widely distributed in the central and peripheral nervous systems and in multiple organs, playing a significant biological role in regulating numerous physiological processes such as motor control, homeostasis regulation, feeding, higher cognitive functions like attention and memory, anxiety, mood, appetite, reward circuits, pain perception, sexual functions, neuroprotection, the immune system, and endocrine functions [25, 26].

The neuropharmacology of CB1 and CB2 receptors is particularly complex and includes not only their action on the ECS but also describes effects on other neurotransmitter systems such as dopamine, glutamate, and gamma-aminobutyric acid (GABA).

CB1 and CB2 belong to the G protein-coupled receptor (GPCR) family, mediating the functional responses of endocannabinoids and exogenous molecules. They are characterized by an amino acid structure that forms a single chain, with the amino-terminal facing the extracellular portion and the carboxyl-terminal protruding into the cytoplasmic membrane. It is ordered into seven transmembrane α -helical domains connected by three extracellular loop segments, which, together with the amino-terminal, compose important glycosylation and ligand interaction

sites, and three intracellular segments that host regulatory sites, serving as sites of interaction with G protein subunits (Fig. 3) [27, 28].

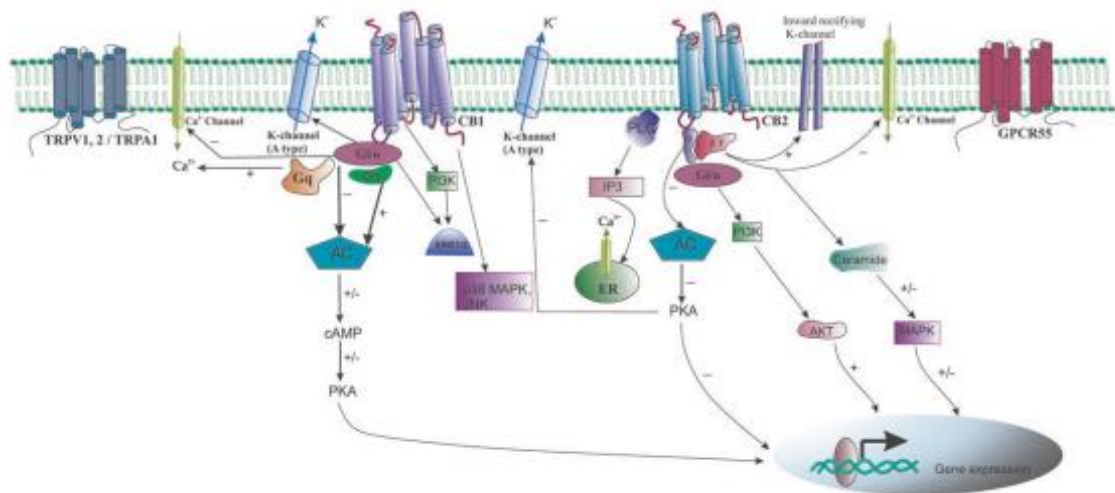


Fig. 3 Schematic representation of the structure and functioning of cannabinoid receptors CB1 and CB2

The CB1 receptors were characterized as cannabinoid binding sites for the first time in 1988 by Devane et al. [29], and a few years later, they were cloned and their structure described in both rats [30] and humans [31]. These receptors are widely distributed in much of the central nervous system and are the most abundant G protein-coupled receptors (GPCRs) in the mammalian brain [32].

Through radiographic, immunohistochemical, and in situ hybridization studies, numerous brain areas such as the olfactory bulb, cerebellum, hippocampus, basal

ganglia, cortex, amygdala, and hypothalamus have been precisely defined as regions where CB1 receptors are particularly expressed [33-35]. A moderate presence of CB1 receptors can be observed in the dorsal horns of the spinal cord, while a lower presence may be found in the ventral horns of the spinal cord and the thalamus [36].

They are also expressed in the peripheral nervous system (PNS) and in numerous tissues and organs, including the immune system, some endocrine glands, the cardiovascular system, the reproductive system, the gastrointestinal tract, and the bone marrow [37-39]. Although CB1 receptors have recently been localized on non-neuronal cells such as astrocytes and postsynaptic neuronal cells, their cellular localization predominantly involves presynaptic areas of neurons, consistent with the neuromodulatory activity typical of these receptors [40, 41].

CB2 receptors, described in 1993 by Munro et al. [42], though sharing structural and, to some extent, signal transduction homologies with CB1, are characterized by a different distribution. They exhibit a high and widespread presence peripherally and an extensive, albeit low, expression throughout the CNS [43]. Peripherally, CB2 receptors are abundantly expressed in immune system cells

such as monocytes, macrophages, B and T lymphocytes, where they participate in inducing the release of pro-inflammatory cytokines and modulate the release of angiogenic and lymphangiogenic factors [44]. These receptors modulate the immune response in other immune-related sites such as the spleen, tonsils, thymus, hematopoietic bone tissue, and keratinocytes [45]. Their presence has also been observed in the pancreas and the gastrointestinal tract [46].

CB2 receptors are expressed in microglia and macrophages of the CNS only in the case of neuroinflammation, suggesting a protective function towards neurons. In case of tissue damage, the up-regulation of the receptor and the subsequent action of endocannabinoids on it lead to a decrease in the release of free radicals and tumor necrosis factor (TNF). This suggests that CB2 receptors may mediate a genuine endogenous protective response to potentially harmful conditions, making them a possible pharmacological target in the treatment of certain neurodegenerative diseases [47]. Furthermore, although the effects associated with the activation of CB2 in the CNS are not yet entirely clear, their involvement in behavioral disorders and substance abuse has been hypothesized [48, 49].

A graphical representation of the distribution of CB1 and CB2 receptors is shown in Figure 4 (Fig.4).

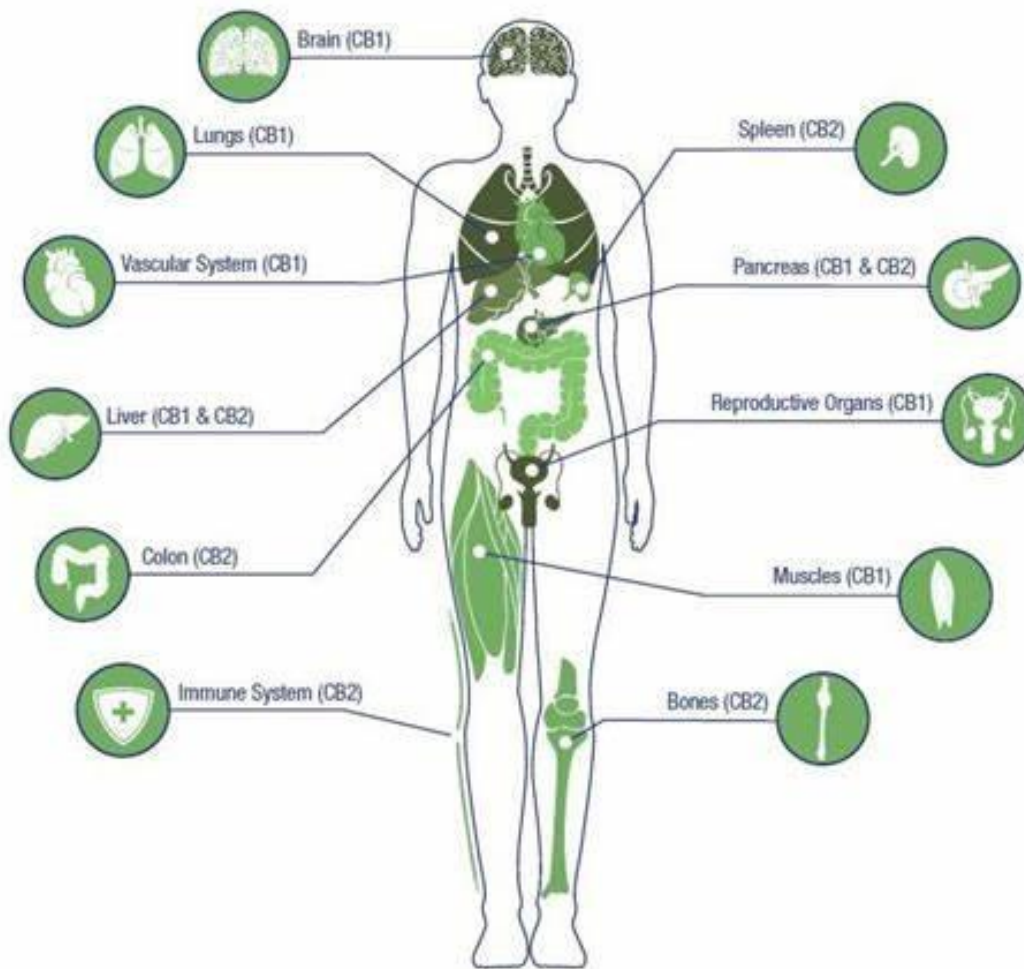


Fig. 4 Graphical representation of the distribution of CB1 and CB2 receptors

The activation of receptors, mediated by Gi and Go proteins, results in the inhibition of adenylate cyclase and, consequently, cAMP, which interacts with calcium and potassium channels, leading to an overall decrease in intracellular

calcium concentrations and extracellular potassium, resulting in reduced neurotransmission. Depending on the specific location of CB and the G protein involved, receptor stimulation can lead to the inhibition or stimulation of various neurotransmitters, including acetylcholine, L-glutamate, GABA, dopamine, norepinephrine, and 5-hydroxytryptamine (serotonin) [50-52].

Discoveries related to the substantial volume of studies conducted from the moment of their discovery to the present day identify CB1 and CB2 receptors as the main mediators of the physiological effects of the ECS. However, in recent years, a proposal, supported by increasing evidence, suggests that other receptors also contribute to the modulation of the ECS. Scientific evidence suggests the interaction of endocannabinoids with other receptor structures such as GPR55 [53] and the transient receptor potential vanilloid type-1 (TRPV1) channel receptor [54]. Additionally, the ECS interacts with the serotonin system: it has been demonstrated that the activation of serotonin receptors can activate the endocannabinoid system. Finally, the activation of G protein-coupled AT1 angiotensin receptors can lead to the stimulation of CB1 receptors, thus regulating blood pressure in the hypothalamus [55].

In summary, it is evident that the activation of CB1 and CB2 receptors by endogenous and exogenous ligands causes a broad spectrum of biochemical responses at the cellular level, leading to the central and peripheral effects observed in cannabinoid toxicity. The discovery of CB receptors, driven by numerous studies aimed at understanding the mechanism of action of Cannabis, immediately sparked strong interest in THC-like molecules presumed to be their endogenous ligands. This drive led Devane et al. as early as 1992 to isolate, from extracts of porcine brain, a lipid molecule identified as arachidonic acid amide (N-arachidonylethanolamide), later named anandamide (AEA) from the Sanskrit "ananda" (meaning a state of grace or bliss), which showed high affinity for CB receptors [56].

A few years later, the second endogenous ligand, also lipidic, was isolated and named 2-arachidonoylglycerol (2-AG) [57]. Today, we know that this class also includes other compounds discovered in the early 2000s, such as 2-arachidonylethanolamine (2-AGE or noladin ether), O-arachidonylethanolamine (virodhamine), and N-arachidonoyldopamine (NADA), all capable of interacting

with CB receptors, although AEA and 2-AG remain the most important endocannabinoids [58-60].

In addition to being partial agonists of CB1 and CB2 receptors, both THC and CBD have a more complex mechanism of action and activate the ECS through different pathways. However, as previously mentioned, CBD is also a negative allosteric modulator of the CB1 cannabinoid receptor. Therefore, when CBD and THC are co-administered, CBD appears to reduce the psychoactivity and anxiogenic effects of THC [61].

2.5 Effects of Cannabis, Semi-synthetic, and Synthetic Cannabinoids

The effects resulting from the recreational use of cannabis are primarily related to the binding of THC to the CB1 receptor and are well-known to the scientific community. The main characteristic of recreational cannabis use is the production of a euphoric or “high” effect [62].

It is well-established that THC possesses anxiolytic, sedative, and analgesic properties. Additionally, it stimulates appetite and can alter the perception of reality, as seeing brighter colors, hearing vivid music, and feeling heightened emotional involvement. However, cannabis use can also lead to dysphoric

reactions, including severe anxiety, panic, paranoia, psychosis, and hallucinations. These reactions, often dose-dependent, exhibit significant interindividual variability and are more common in inexperienced and occasional users, anxious individuals, and psychologically vulnerable individuals [63].

Regarding cognitive and psychomotor performance, the effects include slowed reaction times, motor coordination impairment, specific short-term memory defects, difficulty concentrating, and attention issues, especially in performing complex tasks.

Chronic cannabis use can lead to tolerance, dependence, withdrawal syndrome, and potential long-term cognitive impairment. There is substantial evidence that the cognitive performance of chronic users remains compromised even when not under the substance's influence. These impairments, especially in attention, memory, and the ability to process complex information, can persist for weeks, months, or even years after cessation of use [64].

Tolerance develops to many cannabis effects, and chronic use can lead to withdrawal syndrome characterized by restlessness, insomnia, anxiety, increased aggression, anorexia, muscle tremors, and autonomic effects [65].

The acute toxic effects of cannabinoids are secondary to the overstimulation of the ECS by exogenous cannabinoids. This excessive stimulation leads to irregular modulation of neurotransmitters, resulting in toxicity. The absorption kinetics of cannabinoids and THC depend on the exposure route, with inhalation reaching peak serum concentration in less than thirty minutes and ingestion reaching peak concentration approximately 2-4 hours after consumption. The duration of toxicity from inhalation and ingestion lasts roughly from 2 to 6 hours and 8 to 12 hours, respectively [66].

Regarding acute toxicity, cannabinoids produce cardiovascular effects such as dose-dependent tachycardia, blood pressure changes, neurological effects like drowsiness, ataxia, speech difficulties, widespread vasodilation, conjunctival redness, nystagmus, tachypnea, and bradypnea. Gastrointestinal effects include dry mouth and increased appetite, and postural hypotension and syncope may occur [63, 65, 67].

As previously mentioned, there is significant inter-individual variability in metabolism and effects resulting from Cannabis intake, and since there is no clear

demarcation between doses that achieve desired psychoactive properties and those producing harmful effects, recreational use often results in toxicity [68].

However, such effects are generally self-limiting, and acute toxicity, although frequently encountered, is not generally associated with severe side effects or cases of death.

Unlike THC, which is a well-known molecule and even when used recreationally has a relatively broad safety margin, the effects of semi-synthetic and synthetic cannabinoids, especially when used at high doses, are not yet well-known to the scientific community. Therefore, in addition to the lack of therapeutic utility, their intake can lead to a series of health-threatening side effects [69, 70]. In fact, while THC is a partial agonist of the CB1 receptor, new synthetic molecules may have markedly higher affinity for the receptors, causing more potent toxicological effects than THC [71]. Specifically, synthetic cannabinoids can be non-selective or highly selective agonists of CB1 and/or CB2 receptors, and almost all have a binding affinity much higher than THC or endocannabinoids [17, 72].

From several reports, the effects of synthetic cannabinoids are similar to those caused by Cannabis consumption. Their intake can generate, approximately ten

minutes later, tachycardia, xerostomia, conjunctivitis, and an alteration of perception and mood; these effects can last for about six hours [73].

However, the effects of synthetic cannabinoids can be more severe than those resulting from Cannabis intake, as documented by numerous cases in Europe of individuals arriving at the Emergency Room after consuming "herbal mixture" with cardiovascular and nervous system disorders, such as tachycardia and temporary loss of consciousness.

In confirmation of this, there are reports in the literature of acute intoxications with variable psychiatric manifestations in duration and severity [74], respiratory depression [75], acute myocardial infarction [76], nephrotoxicity [77], gastrointestinal problems such as hyperemesis [78], severe rhabdomyolysis [79], and cerebral ischemia [80].

Regarding semi-synthetic cannabinoids, specifically HHC, toxic effects on humans have not been studied, although recent anecdotal reports from consumers describe effects similar to those of Δ^9 -THC. These effects, like all other cannabinoids, can vary depending on individual tolerance, the quantity and quality of HHC, as well as the method of intake [15].

2.6 Legislative aspects

Due to the psychoactive effects, including potential dependence and abuse, Cannabis and its products are classified as controlled substances in many countries, and their possession is illegal. Currently, in Italy, high-THC Cannabis is illegal for recreational use. In contrast, there are no laws prohibiting CBD, although it is not yet registered as a medicinal product. Because of this legislative gap, some specialty shops offering hemp-derived products freely provide CBD-based items (oil, crystals, etc.) [81].

On the other hand, synthetic cannabinoids constitute the largest group of substances monitored as New Psychoactive Substances (NPS) by the Early Warning System of the European Union. Despite concerted efforts to reduce their availability in the drug market, synthetic cannabinoids gained widespread popularity and distribution in Europe. In Italy, synthetic cannabinoids are listed in Table I of narcotic and psychotropic substances, as per the decree of the President of the Republic on October 9, 1990, no. 309, and subsequent modifications and integrations.

As for HHC, it was the first semi-synthetic cannabinoid reported in the EU in 2022. It has been identified in two-thirds of the Member States and, in some countries, is sold as "Cannabis light," or a legal alternative to Cannabis. Since October 2022, HHC has been intensively monitored by the Early Warning System of the EU to better understand its effects and potential public health risks. Furthermore, in April 2023, the EMCDDA published a technical report on the substance HHC, describing its effects as almost overlapping with those of THC and confirming its alarming spread in the European market.

In line with this evidence, with the Decree of the Ministry of Health on July 13, 2023, published in the Official Gazette attached to this chapter (GU Serie Generale n.172 dated 25-07-2023), the tables of narcotic and psychotropic substances were updated, including HHC and two of its derivatives, HHC-acetate (HHCO), and hexahydrocannabinofuranol (HHCP) in Table I. This decision takes into account the amount of seizures made in Italy in 2022, particularly in the Province of Bolzano, Puglia, Piedmont, and Lombardy, along with numerous reports received between the end of 2022 and the beginning of 2023 from the Unit of Coordination of the National Early Warning System (SNAP) of the Department of Anti-Drug

Policies (DPA), and finally, the favorable opinions of the Higher Institute of Health (ISS) and the Higher Health Council.

3. HEXAHYDROCANNABINOL

3.1 History and diffusion

HHC was first identified in the 1940s during investigations aimed at elucidating the chemical structure of the psychoactive constituents of marijuana and hashish in the laboratories of Adams et al. and Todd et al. [82-84]. Molecular characteristics such as chemical instability, predisposition to isomerization, and the lack of adequate analytical techniques subsequently hindered a more in-depth scientific understanding. In the following years, only a few studies were conducted on animals, while studies on the pharmacology and toxicology of HHC in humans have not yet been carried out.

HHC is naturally found in small concentrations in the pollen and seeds of hemp plants, and it is chemically similar to Δ^9 -THC. According to laboratory studies in vitro and on some animal species in vivo, HHC appears to have substantially similar effects to Cannabis-based products [15].

Recently, due to its rapid spread and popularity as a substance of abuse, HHC has once again captured the attention of researchers and toxicologists internationally.

Indeed, in the early 2000s, a crisis occurred in the global illicit cannabinoid market, and, parallel to legislative changes, semi-synthetic and synthetic cannabinoids emerged in the market—economical and easy to produce. This proliferation is linked to regulatory changes in the United States concerning the legal status of hemp. The enactment of the Agriculture Improvement Act in 2018, commonly known as the "Farm Bill," opened the doors to large-scale cultivation of industrial hemp and “low-THC cannabis” [85].

The hemp and derivative market, for both therapeutic and recreational purposes, has grown exponentially. Consequently, with increased supply, prices of many products have decreased, and products containing hemp derivatives (especially CBD or low-THC cannabis) have proliferated in the market without legislative restrictions.

HHC is openly sold as a "legal" substitute for THC-based products, often in the form of vaporizers or liquid substances intended for electronic cigarettes, as well as

in food products such as sweets or candies. Even now, in many countries, it is freely distributed as "cannabis light." Marketing operations and advertisements often directly compare or allude to similarities in the effects of these substances [86, 87]. HHC appeared in the U.S. narcotics market in 2021. Subsequently, around May 2022, it was first identified in Europe, found in food product marketed as a sleep aid called "CBN night," seized by the Danish police (Fig.5) [88].



Fig. 5 The “CBN night” seized by the Danish police

In a short period, the production and distribution of HHC began affecting other countries, and between 2022 and 2023, the European Monitoring Centre for Drugs and Drug Addiction (EMCDDA) received various reports through the EU early warning system regarding new psychoactive substances (NPS) where HHC was identified in a range of products in 20 EU member states (Austria, Belgium,

Bulgaria, Croatia, Cyprus, Czech Republic, Denmark, Estonia, Finland, France, Germany, Greece, Hungary, Italy, Lithuania, Poland, Slovakia, Slovenia, Spain, Sweden), Switzerland, and Norway (Fig. 6). Therefore, the need for careful monitoring was highlighted, and in some countries, legal status changes have already occurred [88].

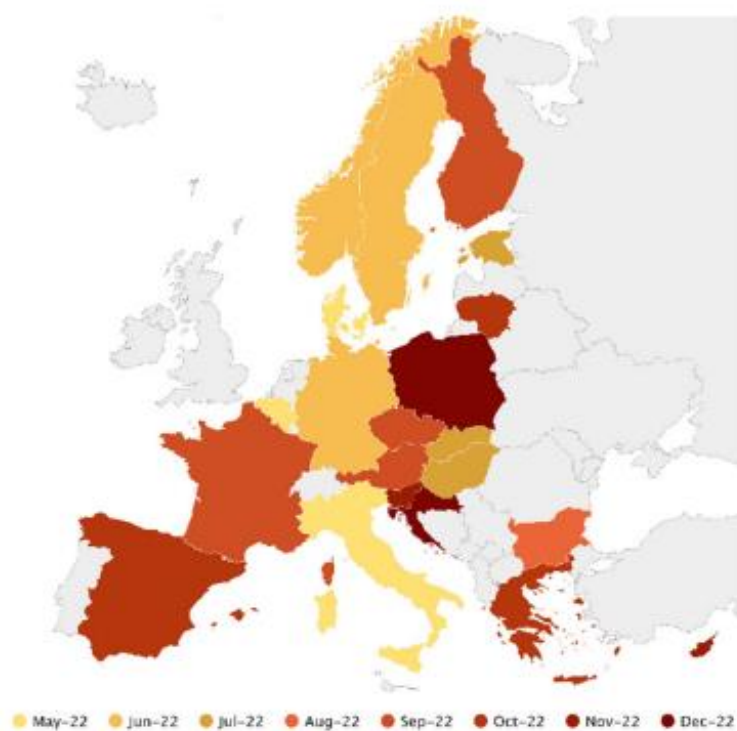


Fig. 6 European countries reporting identifications of HHC to the EWS (May-December 2022) EMCDDA 2023

Since its formal notification as an NPS, the EMCDDA has received reports of about 50 seizures. Monitoring data suggests that the availability and use of HHC in

Europe are much higher, and there is a wide range of products on the market where the packaging indicates the presence of HHC; furthermore, some are sprayed or mixed with HHC even though its presence is not reported (often low-THC cannabis flowers and resin).

Products are marketed using popular names of Cannabis varieties like “Afghan Kush”, “Amnesia”, “BubbleGum Kush”, “Strawberry Kush”, “Express”, and “Purple Haze” (Fig. 7), as well as e-cigarette liquids (Fig. 8), food products, especially flavored sweets (gummies and marshmallows) (Fig. 9 and 10), and blends marketed as dietary supplements [88].



Fig. 7 Packaging of “Purple Haze” containing low-THC cannabis flowers containing HHC,

EMCDDA 2023.



Fig. 8 Liquid packaging for electronic cigarettes containing HHC, EMCDDA 2023.



Fig. 9 Packaging of gummy candies flavored “Coke” containing HHC, EMCDDA 2023.



Fig. 10 Packaging of strawberry-flavored marshmallows containing HHC, EMCDDA 2023.

These items are sold in physical stores specializing in the sale of light Cannabis but primarily online. In fact, in recent years, there has been a significant increase in distribution and sales, particularly through dark and deep web websites. This has opened the market to a large number of potential consumers, including not only regular Cannabis users but also new consumers such as adolescents or individuals with no experience with illicit substances who are attracted by the legal status of HHC, as many countries still allow its legal intake. Despite the lack of in-depth studies on the activity, potency, toxicity, and safety of HHC, this cannabinoid is increasingly used by the hemp-derived product industries.

From a clinical perspective, the effects of HHC seem to be similar to those experienced by Cannabis users and other THC-based products. However, since the pharmacokinetics, metabolism, and toxicity of this substance are not currently known, it cannot be ruled out that HHC may have greater side effects than THC-based products.

From the analysis of marketed products, it emerges that these preparations contain two stereoisomers of HHC, namely, 9R-HHC and 9S-HHC. According to non-clinical studies, pharmacological properties similar to Δ^9 -THC are attributed, in particular, to 9R-HHC. Laboratory studies have indeed shown that the 9R-HHC epimer has a higher affinity for endocannabinoid receptors than the 9S-HHC epimer and, consequently, seems to determine psychoactive effects similar to THC. The actual content of HHC, especially of its epimers, in marketed products is not regulated and is highly variable. The HHC distributed in the market is, in fact, a mixture of both epimers in proportions not always known, resulting in variability in clinical and side effects [88].

3.2 Name, Structure, and Chemical Properties

Hexahydrocannabinol (IUPAC name: 6a,7,8,9,10,10a-hexahydro-6,6,9-trimethyl-3-pentyl-6H-dibenzo[b,d]pyran-1-ol, HHC) is a hydrogenated derivative of Δ^9 -THC; it is a phytocannabinoid present in very small quantities in *Cannabis sativa*, as well as a synthesis product derived from the hydrogenation of *Cannabis* [89]. HHC is produced from THC following the hydrogenation process of the C9-C10 bond in the cyclohexyl ring (Fig.11) [90].

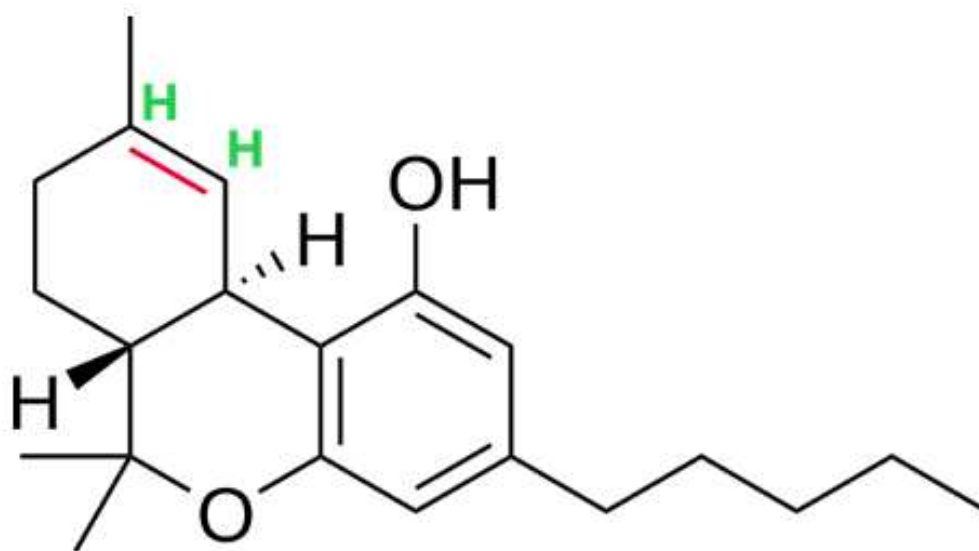


Fig. 11 Chemical structure of HHC: Unlike THC, it features two Hydrogen (H) atoms (in green) and the loss of the double bond C9-C10 (in red).

The HHC molecule contains three stereogenic centers with eight possible stereoisomers, as reported in the reference literature. Only the carbon in position

C9 shows both configurations ((6aR,9S,10aR)-HHC or 9 α -HHC and (6aR,9R,10aR)-HHC or 9 β -HHC), respectively called 9S-HHC and 9R-HHC [91].

The chemical structure and molecular formula of the two HHC epimers are shown in Figure 12 (Fig.12).

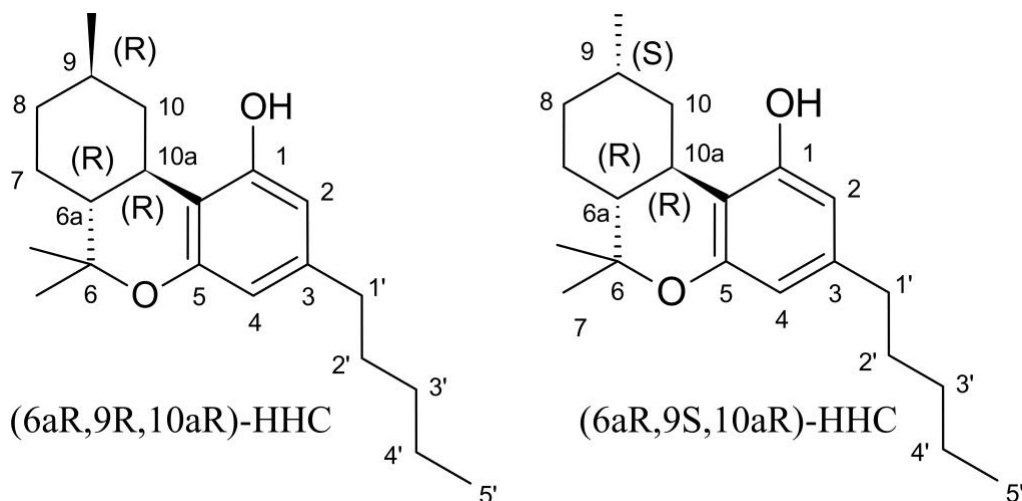


Fig. 12 Chemical structure and molecular formula of 9R-HHC (left) and 9S-HHC (right).

Between the two isomers, the only difference is the spatial position of the methyl group at C9, which is axial in 9S-HHC, whereas it is equatorial in 9R-HHC, i.e., essentially the same position as the C9 methyl of Δ 9-THC (Fig. 13). In Figure

14, the overlapping three-dimensionality of the two HHC epimers and Δ^9 -THC is appreciable (Fig.14).

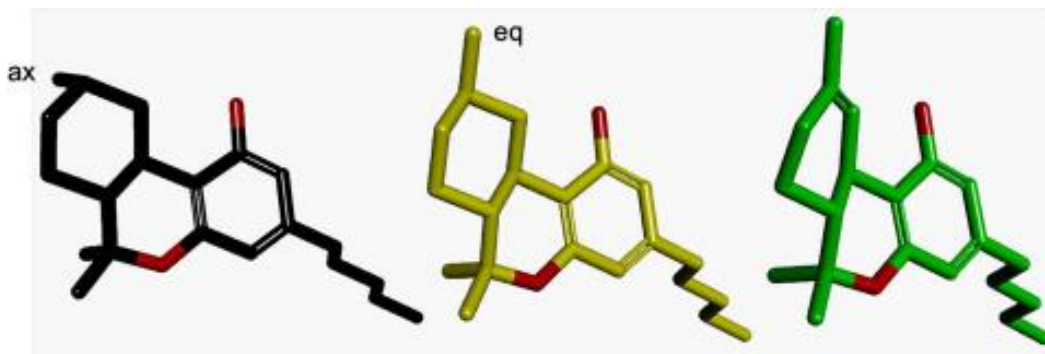


Fig. 13 Three-dimensional structure of 9S-HHC (in black), 9R-HHC (in yellow), and THC (in green).

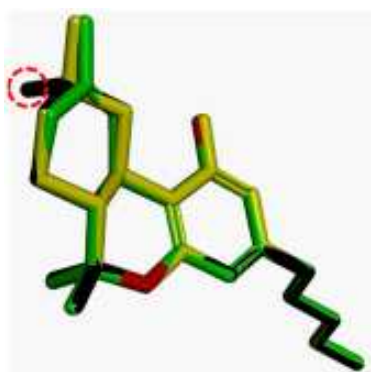


Fig. 14 The overlap of the three cannabinoids: it can be observed that the two isomers differ only in the spatial position of the C-9 methyl group, which in 9S-HHC (black) is axial (marked by a red circle), while in the 9R-HHC epimer (yellow) it is equatorial, essentially overlapping the position of the C-9 methyl in Δ^9 -THC (green). [Created by István Ujváry using BIOVIA Studio Visualizer. EMCDDA 2023].

As mentioned earlier, *in vitro* studies have suggested that the 9R-HHC epimer has superior psychoactive activity to the 9S-HHC epimer; indeed, 9R-HHC appears to exert cannabimimetic activity, while 9S-HHC seems to have less psychotropic activity [92, 94].

Few *in vivo* studies are available in the literature, and only on animals. Of these, it is worth mentioning the work conducted by Edery et al., whose objective was to evaluate the psychotropic activity of HHC epimers on rhesus monkeys after the administration of the two single epimers, by observing any somatic and behavioral changes. The authors observed that after the administration of 1 mg/kg of 9R-HHC, the monkeys remained in a state of severe stupor, characterized by ataxia, complete ptosis, and immobility for more than 3 hours, with a total lack of reaction even in the presence of external stimuli. These effects gradually decreased at lower doses, observing only a state of tranquility at doses of 0.1 mg/kg. On the other hand, the 9S-HHC epimer induced drowsiness, decreased motor activity, and occasionally, partial ptosis at higher doses, equal to 5 mg/kg [95].

In a recent study by Russo et al., the cannabinoid activity of the two HHC epimers in mice was compared. In detail, it was shown that the intraperitoneal

administration of 10 mg/kg of 9R-HHC reduced spontaneous motor activity and induced catalepsy, analgesia, and hypothermia. The same effects were not observed in mice that received the same dose of 9S-HHC, which showed no alteration in locomotion, nor catalepsy and analgesia [96]. These data suggest that the presence, in HHC-based products, of different concentrations of one epimer compared to the other, leads to high variability in both recreational and side effects [93].

3.3 Synthesis of HHC

HHC is not biosynthesized by hemp; however, small traces have been detected in hemp extracts as degradation products of Δ^9 -THC. For this reason, HHC has been considered a semi-synthetic phytocannabinoid.

HHC can indeed be produced from chemical precursors obtained from hemp or through total synthesis. The main methods of HHC production involve the direct reduction of Δ^9 -THC (as well as Δ^8 -THC), but it can also be produced following acid treatment and subsequent hydrogenation of cannabidiol (CBD) [97].

In practice, HHC is mainly produced through the hydrogenation process of THC, which involves adding pressurized hydrogen to THC present in the Cannabis extract. As mentioned earlier, this breaks the double carbon bond, and two

hydrogen atoms are bonded, creating a dense oil called "hydrogenated cannabis oil" [98].

When synthesized from CBD extracts, a preliminary step involving acid catalysis with the formation of Δ^9 -THC and Δ^8 -THC is required. Subsequent hydrogenation leads to the formation of the two epimers 9R-HHC and 9S-HHC (Fig.15). The reduction reaction, to accelerate and promote the subsequent hydrogenation process, can be catalyzed by various molecules, including platinum, palladium, or iridium [99, 100]. The most commonly used solvents for hydrogenation, typically conducted at atmospheric pressure, are ethanol and acetic acid.

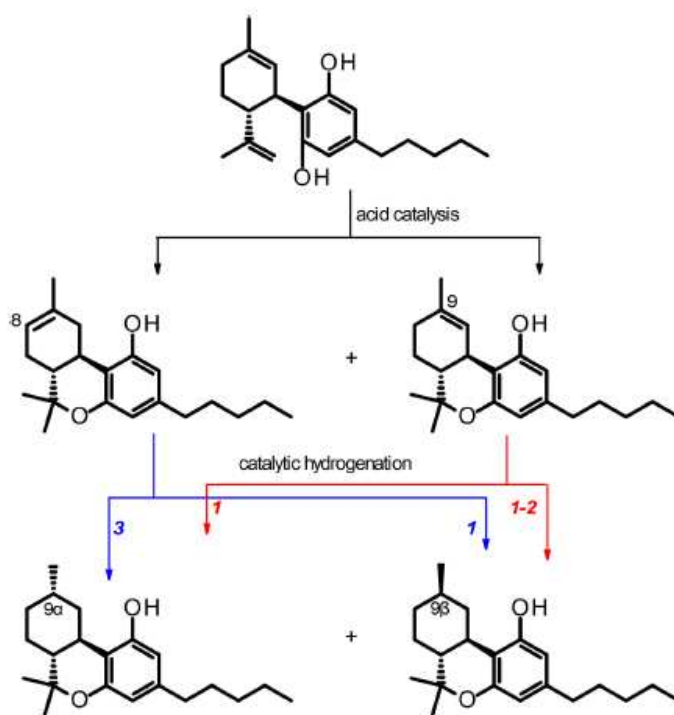


Fig.15 Diagram of the synthesis of HHC starting from CBD. The numbers in red and blue indicate the approximate proportions of the HHC epimers produced by the hydrogenation of the respective THC isomers.

The hydrogenation of the THC isomer mixture provides the 9R-HHC and 9S-HHC epimers based on the isomeric composition of the initial THC mixture and the catalyst used. For example, hydrogenation of Δ^9 -THC using a platinum catalyst yields 9S-HHC and 9R-HHC in an approximately 1:2 ratio.

In contrast, hydrogenation of Δ^8 -THC using the same catalyst favors the production of the 9S-HHC isomer over the 9R-HHC isomer in a ratio of 3:1 or 3:2 [101, 102].

The semi-synthetic HHC currently marketed is typically a mixture of the 9S-HHC and 9R-HHC epimers. However, large-scale hydrogenation of THC or CBD mixtures provides variable concentrations of the two epimers, and therefore, products with varying percentages are marketed between different batches [103].

4. OBJECTIVES OF THE RESEARCH

The pharmacotoxicological properties and pharmacokinetics of HHC are not yet fully understood, and individuals consuming HHC are not aware that this substance may have toxic effects similar to or even greater than common THC. Based on these assumptions, further studies on the metabolism of HHC, its stereoisomers, and their respective metabolites, as well as new in-depth studies on the pharmacokinetics of semi-synthetic cannabinoids in humans, are essential.

Due to the lack of in-depth studies on this molecule, which is spreading worldwide, many EU countries have decided to ban the use of HHC. In particular, Austria, Finland, and Estonia were the first European countries to impose bans on the production, sale, and use of HHC, including as a liquid in electronic cigarettes. They were followed by Sweden, Belgium, Denmark, the United Kingdom, and France. In Italy, as of July 13, 2023, HHC has been included in Schedule I of controlled substances (Decree 309/90 of the Ministry of Health).

However, the rapid and growing popularity of HHC worldwide, its structural similarity to THC, and the lack of currently available scientific data make further scientific studies necessary and essential.

To date, there are very few studies on the pharmacokinetics of HHC and its stereoisomers, some of which are in vitro and others in vivo on animals, but only one was conducted in human biological matrices of two subjects.

The first objective was to assess the metabolism of HHC and to identify the main consumption biomarkers both through in silico prediction and through incubation of the substance with human hepatocytes.

The second goal was to develop and validate an analytical method in ultra-high-performance liquid chromatography coupled with tandem mass spectrometry (UHPLC-MS/MS) for the determination and quantification of HHC and its main metabolites. Simultaneous characterization of its two stereoisomers, 9R-HHC and 9S-HHC, in biological matrices was also a goal.

The final aim of the research was to study the clinical effects and pharmacokinetics of HHC in humans. To achieve this, blood, urine, and oral fluid samples were collected from 7 healthy volunteers after a controlled consumption of a single cigarette containing 500 mg of tobacco mixed with 25 mg of HHC.

Finally, the obtained data were compared with those present in the literature, and the main differences between the 9R- and 9S-HHC isomers were evaluated.

5. IN SILICO AND IN VITRO METABOLISM

5.1 Materials and Methods

In silico prediction of metabolites was carried out using specific software BioTransformer (University of Hamburg, Germany).

The two epimers, 9S-HHC and 9R-HHC, were mixed with a pool of human hepatocytes from 10 donors and left to incubate for 3 hours. In order to exclude interferences due to non-enzymatic reactions, “negative controls” were performed by respectively excluding hepatocytes and the substance to be analyzed.

Following deproteinization, the incubates were analyzed using liquid chromatography coupled with high-resolution mass spectrometry (HRMS/MS-MS) through a complete data scan (full scan - Q-Exactive, Thermo Scientific). The obtained results were processed using dedicated software (Compound Discoverer, Thermo Scientific).

The results obtained were also compared with those from urine samples taken from three female volunteers aged from 26 to 49, who declared themselves occasional recreational users of HHC.

5.1.1 In silico predictions

HHC metabolites were predicted with BioTransformer open-access software v.3.0. HHC SMILES string, generated through ChemSketch v.2020.1.2, was input with “AllHuman” and “Combined CYP450” options, to generate a comprehensive list of phase I and phase II putative metabolites within the human superorganism using both a rule-based method and machine-learned model. A maximum number of reaction iterations of 2 was selected.

5.1.2 Chemicals and reagents

The analytical standards 9S- and 9R-HHC were purchased from Cayman Chemical. Diclofenac (used as a positive control), HPLC grade acetic acid, β -glucuronidase from limpets, growth medium (Williams’ medium E, WME), l-glutamine, HEPES (2-[4-(2-hydroxyethyl)-1-piperazinyl]ethanesulfonic acid), HPLC grade ammonium acetate, and LC-MS grade formic acid were provided by Sigma Aldrich. All analytical standards were prepared at a concentration of 1 mg/mL by dilution with appropriate amounts of methanol and stored at -20°C until the time of analysis. Solvents (water, acetonitrile, and methanol) required for the experiments, all of LC-MS grade, were purchased from Carlo Erba.

Pools of human hepatocytes from ten donors and thawing medium were purchased from Lonza (Lonza Italia) and stored in liquid nitrogen until incubation.

5.1.3 Hepatocyte incubation

Hepatocytes were thawed in a water bath at a temperature of 37°C for approximately 90 - 120 seconds and then transferred into a 50 mL conical polypropylene tube containing the thawing medium. The cells were then centrifuged for 5 minutes at 50-100 g at room temperature, and once the supernatant was removed, the cells were resuspended in 50 mL of WME supplemented with 2 mmol/L l-glutamine and 20 mmol/L HEPES (SWME).

After centrifugation for 5 minutes at 50-100 g at room temperature and discarding the supernatant, the cells were resuspended in 2 mL of SWME and counted by exclusion staining with Trypan blue to assess vitality; the volume was adjusted with SWME based on cell vitality to obtain a concentration of 2×10^6 cells/mL. Subsequently, 250 μ L of 20 μ mol/L 9R- or 9S-HHC in SWME was mixed with 250 μ L of the cell suspension and incubated at a temperature of 37°C. The reactions were then interrupted by adding 500 μ L ice-cold acetonitrile at 0 h

(immediately after inoculation) and after 3 h. Incubates were stored at -80°C until analysis.

5.1.4 Sample preparation

After thawing, 100 µL incubate or control was mixed with 100 µL acetonitrile (or 100 µL urine was mixed with 200 µL acetonitrile) and centrifuged for 10 min, 15,000 g. The supernatants were evaporated to dryness under nitrogen, then reconstituted in 100 µL water:acetonitrile 80:20 (v/v) with 0.1% formic acid. After centrifugation for 10 min, 15,000 g, the supernatants were transferred in autosampler vials with a glass insert.

Additionally, 100 µL urine was mixed with 10 µL 10 mol/L ammonium acetate, pH 5.0, and 100 µL β-glucuronidase (5,000 units) and incubated overnight (16 h) at 37°C. After hydrolysis, the sample was vortexed with 400 µL acetonitrile and centrifuged for 10 min, 15,000 g. The supernatants were evaporated to dryness under nitrogen, then reconstituted in 100 µL water:acetonitrile 80:20 (v/v) with 0.1% formic acid. After centrifugation for 10 min, 15,000g, the supernatants were transferred in autosampler vials with a glass insert.

5.1.5 HHC positive urine samples

A urine sample was collected from three different individuals who declared themselves to be occasional recreational users of HHC that had taken the substance in the last 12 hours. Through LC-HRMS/MS analysis, concentrations of 9S- and 9R-HHC were detected at 8.4 and 7.7 ng/ml, 5.1 and 3.9 ng/ml, and 3.7 and 4.5 ng/mL, respectively. No other substances of chemical-pharmacological interest were detected in the first-level screening.

5.1.6 LC-HRMS/MS settings

Extracted samples were stored at $10\pm 1^{\circ}\text{C}$ in the autosampler before injection of 10 μL . The analysis was performed using a Dionex UltiMate 3000 chromatographic system coupled with a Thermo Scientific Q Exactive high-resolution mass spectrometer equipped with an electrospray ionization source.

Chromatographic separation was carried out at $37\pm 1^{\circ}\text{C}$ using a Phenomenex Kinetex Biphenyl column (150 x 2.1 mm, 2.6 μm) with a linear gradient of mobile phase at 0.4 mL/min. Mobile phases A (MPA) and B (MPB) were water and acetonitrile, respectively, both containing 0.1% formic acid.

The ionization source settings were as follows: spray voltage, ± 4.0 kV; sheath gas flow rate, 50 a.u.; auxiliary gas flow rate, 5 a.u.; auxiliary gas temperature,

300°C; capillary temperature, 300°C; -lens radio frequency level, 50 a.u. The mass spectrometer was operated in full-scan MS/data-dependent MS/MS mode from 1 to 23 minutes, and the data were collected using Thermo Scientific Xcalibur software (v. 4.1.31.9).

5.2 Results

At the end of the 3 hours incubation, metabolic activity was assessed through the in vitro formation of metabolites. In particular, hydroxy-(9S)-HHC-glucuronide (S3) and 11-hydroxy-(9S)-HHC-glucuronide (S4) have been identified for 9S-HHC (Fig. 16); dihydroxy-(9R)-HHC-glucuronide (R3) and hydroxy-(9R)-HHC-glucuronide (R7) have been identified for 9R-HHC (Fig. 17).

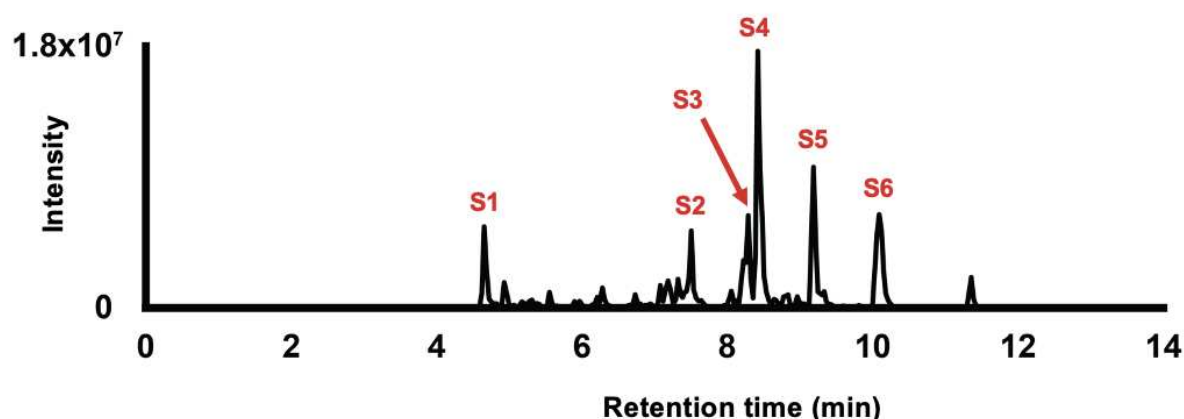


Figure 16: HRMS/MS chromatograms of hepatocytes incubated with 9S-HHC.

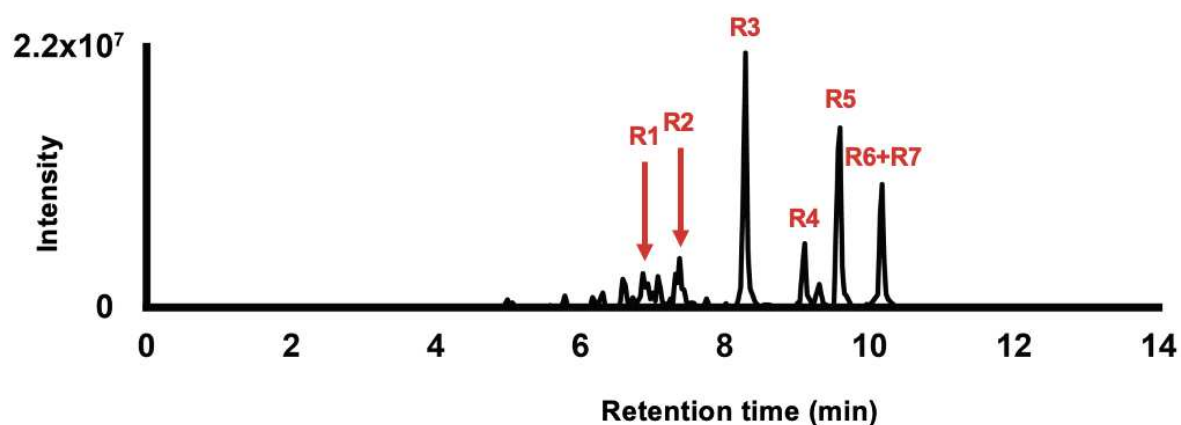


Figure 17: HRMS/MS chromatograms of hepatocytes incubated with 9R-HHC.

The main metabolic reactions observed in the examined biological samples (urine) were oxidation, carboxylation, and glucuronidation, both individually and in combination (Fig. 18 and 19).

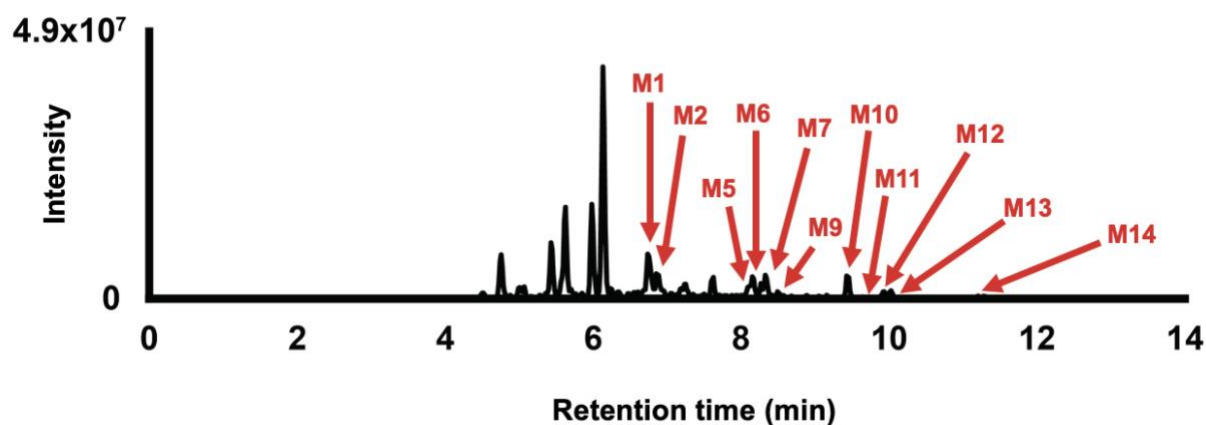


Figure 18: HRMS/MS chromatograms of one urine sample without glucuronide hydrolysis.

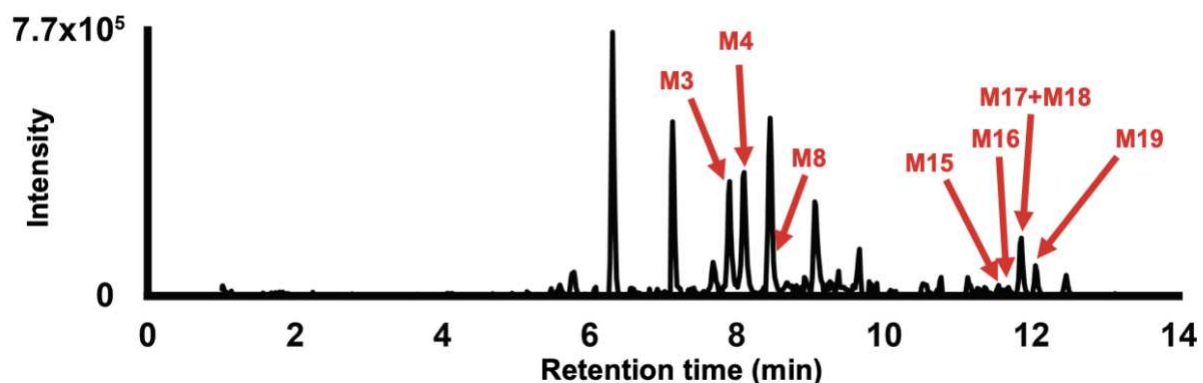


Figure 19: HRMS/MS chromatograms of one urine sample with glucuronide hydrolysis.

HHC was not detected before hydrolysis and was minor after hydrolysis.

In non hydrolyzed urine, primary metabolites of 9S-HHC were hydroxy-(9S)-HHC-glucuronide (M7); primary metabolites of (9R)-HHC were dihydroxy-(9R)-HHC-glucuronide (M1) and hydroxy-(9R)-HHC-glucuronide (M10 – Table 1).

In hydrolyzed urine, primary metabolites were dihydroxy-(9S)-HHC and/or dihydroxy-(9R)-HHC (M3, M4) and hydroxy-(9S)-HHC and/or hydroxy-(9R)-HHC (M16 – Table 2).

11-COOH-S-HHC (M19), 11-COOH-R-HHC (M18), 11-OH-S-HHC or 11-OH-R-HHC (M17), and 9-β-OH-HHC (M15) were detected in hydrolyzed urine, but all as minor metabolites.

8-OH-R-HHC and/or 8-OH-R-HHC was/were also found in some of the hydrolyzed urine samples, but the intensity was below the threshold.

Several glucuronides in the hydrolyzed urine samples were only partially hydrolyzed.

Table 1: Major metabolites in non-hydrolyzed urine.

ID	Transformation	Elemental composition	m/z HESI+ m/z HESI-	RT (min)	Peak area HESI+				
					HEP S- HHC	HEP R- HHC	Sample 1	Sample 2	Sample 3
M1	Hydroxylation (C ₇₋₉ or 11) + Hydroxylation (pentyl) + O- glucuronidation	C ₂₇ H ₄₀ O ₁₀	525.2694 523.2549	6.74	ND	9.5x10 ⁶ 1.7x10 ⁷	1.6x10 ⁶ interfered	1.3x10 ⁷ 2.0x10 ⁷	2.5x10 ⁶ 5.2x10 ⁶
M7	Hydroxylation (C ₇₋₉ or 11) + O- glucuronidation	C ₂₇ H ₄₀ O ₉	509.2745 507.2600	8.35	1.4x10 ⁷ 7.2x10 ⁷	ND	6.8x10 ⁶ 2.5x10 ⁷	5.1x10 ⁶ 1.9x10 ⁷	9.4x10 ⁵ 2.9x10 ⁶
M10	Hydroxylation (C ₇₋₉ or 11) + O- glucuronidation	C ₂₇ H ₄₀ O ₉	509.2745 507.2600	9.46	ND	2.1x10 ⁷ 7.1x10 ⁷	8.7x10 ⁶ 2.6x10 ⁷	6.2x10 ⁶ 1.4x10 ⁷	1.2x10 ⁶ 3.5x10 ⁶

Table 2: Major metabolites in hydrolyzed urine.

ID	Transformation	Elemental composition	m/z HESI+ m/z HESI-	RT (min)	Peak area HESI+				
					HEP S- HHC	HEP R- HHC	Sample 1	Sample 2	Sample 3
M3	Hydroxylation (C ₇₋₉ or 11) + Hydroxylation (pentyl)	C ₂₁ H ₃₂ O ₄	349.2373 347.2228	7.90	ND	ND	2.1x10 ⁶ 5.9x10 ⁵	4.0x10 ⁶ 1.2x10 ⁶	9.2x10 ⁵ 2.4x10 ⁵
M4	Hydroxylation (C ₇₋₉ or 11) + Hydroxylation (pentyl)	C ₂₁ H ₃₂ O ₄	349.2373 347.2228	8.10	ND	ND	1.7x10 ⁶ 6.0x10 ⁵	3.6x10 ⁶ 1.4x10 ⁶	2.6x10 ⁵ 1.0x10 ⁵
M16	Hydroxylation (pentyl)	C ₂₁ H ₃₂ O ₃	333.2424 331.2279	11.61	ND	ND	1.8x10 ⁶ ND	1.9x10 ⁶ ND	2.0x10 ⁵ ND

6. DEVELOPMENT AND VALIDATION OF A STEREOSELECTIVE BIOANALYTICAL METHOD IN UHPLC-MS/MS

6.1 Material and Methods

6.1.1 Chemicals and materials

9R-HHC and 9S-HHC standards and all metabolites (9 β -OH-HHC, 9 α -OH-HHC, 8S-OH-9S-HHC, 8R-OH-9R-HHC, 11-OH-9S-HHC, 11-OH-9R-HHC, 11-Nor-9S-COOH-HHC, 11-Nor-9R-COOH-HHC) were acquired from LGC Standard Ltd (Teddington, UK), THC-d3 standards were purchased from Cerilliant (Round Rock, Texas, USA), Standards were stored at -20°C until their use. LC-MS grade water, methanol, n-hexane, and ethyl acetate were obtained from Auchem instruments (Macerata, Italy). HPLC grade acetic acid was purchased from Sigma Aldrich (Milan, Italy). 8S-OH-9R-HHC and 8R-OH-9S-HHC standards were not commercially available at the time of the analysis.

6.1.2 Calibrators and quality control (QC) solutions

Two different aliquots (I and II) from each standard stock solution were prepared. Calibrators were made from aliquot I standard stock solution containing all analytes at 10 and 100 ng/mL in methanol. Aliquot II (10 and 100 ng/mL) were used to prepare quality controls (QCs). THC-d3 (internal standard) stock solution was prepared with the same procedure mentioned above at 100 and 1000 ng/mL concentrations and stored in glass vials at -20°C until use. Blank human whole blood, urine and oral fluid samples were provided by the University Politecnica delle Marche storehouse (Ancona, Italy). The calibrators and QC samples were prepared by spiking pooled blank matrices of blood, urine and oral fluid which were prepared from authentic samples tested negative for the analytes of interest and the most common drugs of abuse.

Based on an initial semi-quantitative analysis of authentic blood, urine and oral fluid samples, the following calibrators were prepared: 0.25, 0.5, 1, 2.5, 5, 7.5, 15, 30, 60, 120, 240 ng/mL for 9R-HHC and 9S-HHC. For 9R-HHC and 9S-HHC low-, medium-, and high-QC samples were 0.75, 96 and 192 ng/mL, respectively. In the case of HHC metabolites following calibrators were prepared: 1, 2.5, 5, 10, 25, 50,

100 ng/mL, low-, medium-, and high-QC samples were 3, 40 and 80 ng/mL, respectively.

6.1.3 HHC on positive samples

Blood, urine, and oral fluid samples were collected from two male volunteers aged 33 and 35, who declared themselves occasional recreational users of HHC. The subjects had consumed controlled doses (25 mg) of the 9R-HHC and 9S-HHC mixture through inhalation in the preceding 3 hours. All subjects had provided written informed consent, and the study was conducted in accordance with the Declaration of Helsinki and approved by the Institutional Ethics Committee (IRCCS- INRCA Ancona). Both volunteers had undergone pharmacological urine screening the previous day (using the Dionex UltiMate 3000 chromatographic system coupled with a Thermo Scientific Waltham, MA, USA Q Mass Spectrometer – LC-HRMS/MS), which was negative for the most common drugs of abuse (opioids, cocaine, cannabinoids, and amphetamines).

6.1.4 Sample preparation

6.1.4.1 Blood and oral fluid

A volume of 10 μL of the 1 $\mu\text{g}/\text{mL}$ internal standard (THC-d3), 200 μL of H_2O and 1 mL n-hexane: ethyl acetate 9:1 (v/v) with 10% of acetic acid were added to 100 μL of blood or oral fluid samples. The tubes were stirred using a roller mixer for 30 min and centrifuged at 2800 rpm for 15 min. Supernatants were transferred into clean tubes and dried under nitrogen at 40-50°C, for 30 min. Samples were reconstituted in 100 μL of methanol and transferred into autosampler vials, prior to injection of 1 μL onto the chromatographic system.

6.1.4.2 Urine

A volume of 10 μL of the 1 $\mu\text{g}/\text{mL}$ internal standard (THC-d3) and 20 μL of 5 mol/L NaOH were added to 100 μL of urine samples for hydrolysis at 70°C for 30 minutes. Then, 1 ml of 5 mol/L ammonium formate, 20 μL of formic acid (pH 4) and 3 ml n-hexane:ethyl acetate 9:1 (v/v) were added. The tubes were stirred using a roller mixer for 10 min and centrifuged at 3500 rpm for 5 min. Supernatants were transferred into clean tubes and dried under nitrogen at room temperature for approximately 30 min. Samples were reconstituted in 100 μL of methanol and

transferred into autosampler vials, prior to injection of 1 μL onto the chromatographic system.

6.1.5 High-performance liquid chromatography tandem mass spectrometry (HPLC-MS/MS) analysis

Following chiral and achiral columns were screened for separation of HHC epimers and their metabolites in this study: Lux Amylose-2 (amylose tris(5-chloro-2-methylphenylcarbamate), Lux i-Amylose-3 (amylose tris(3-chloro-5-methylphenylcarbamate) (250 x 4.6 mm, 5 μm), Lux AMP with a proprietary chiral selector (150 x 4.6 mm, 3 μm), two achiral (Kinetex[®] biphenyl and Kinetex[®] phenyl-hexyl; 100 x 2.1 mm, 2.6 μm) columns from Phenomenex Inc. (Torrance, CA, USA) and Chiralpak AY-3 (amylose tris(5-chloro-2-methylphenylcarbamate) (150 x 4.6 mm, 3 μm) (Daicel, Tokyo, Japan). Methanol was used as a mobile phase for chiral columns. In case of achiral columns two different mobile phases were used for separation of HHC and their metabolites, one pure methanol and second mobile phase was composed with mobile phase A: 5 mmol/L ammonium formate in water and mobile phase B: Methanol + 0.1% formic acid (FA).

A HPLC 1290 Infinity II (Agilent Technologies Italia S.p.a., Milan, Italy) coupled to a mass spectrometer (6470A Triple Quadrupole LC-MS) equipped with an electrospray ionization source (ESI) operated in both positive and negative mode was used. Data were acquired with MassHunter® Workstation Quantitative Analysis 10.0 Software (Agilent). Using the MassHunter Optimizer® program provided by Agilent, the optimization procedure was carried out automatically and manually verified. Separation of HHC stereoisomers was performed on Lux i-Amylose-3 column. Run time was 11 min with an isocratic mobile phase composed of methanol. For separation of the metabolites Lux AMP chiral column was used with 16 minutes run time, isocratic mobile phase was composed of methanol and water 80:20 (v/v). Autosampler and column oven temperatures were 10°C and 25°C, respectively. The mass spectrometer was operated in scheduled multiple reaction monitoring (MRM) mode, with two transitions for each analyte and internal standard (Table 3). MS parameter settings were optimized by infusing neat standards (100 ng/mL) individually in methanol and ramping cone voltage and collision energy. Scan speed (dwell time) was 0.023 sec. ESI conditions were

optimized as follows: capillary voltage 3500 V, source temperature 300°C, cone gas flow rate 10 L/min, desolvation gas flow rate 12 L/min.

Table 3: Mass spectrometry parameters for analytes and internal standards with positive and negative ionization.

Abbreviations: THC, delta-9-tetrahydrocannabinol; HHC, hexahydrocannabinol; CE, collision energy; ESI, electrospray ionization.

Analytes	Molecular mass (g/mol)	Precursor ion (m/z)	Product ion (m/z)	Retention time (min)	CE (eV)	ESI
THC-d ₃	317.49	318.49	196.2	2.56	25	+
			126.1		37	
9R-HHC	316.48	317.48	193.2	7.67	28	+
			123.2		40	
9S-HHC	316.48	317.48	193.2	8.56	24	+
			123.2		36	
11-Nor-9R-COOH-HHC	346.5	345.5	301.3	9.2	24	-
			191.2		37	
11-Nor-9S-COOH-HHC	346.5	345.5	327.4	13.6	24	-
			191.2		44	
11-OH-9R-HHC	332.4	331.4	301.4	10.4	28	-
			191.2		40	
11-OH-9S-HHC	332.4	331.4	301.3	12.3	32	-
			191.2		40	
8R-OH-9R-HHC	332.4	331.4	233.3	12.3	32	-
			95.1		44	
8S-OH-9S-HHC	332.4	331.4	233.3	10.6	32	-
			95.1		44	
9 α -OH-HHC	332.4	331.4	313.4	12.9	28	-
			205.2		32	
9 β -OH-HHC	332.4	331.4	313.3	7.6	24	-
			205.2		32	

6.2 Method validation

Analytical bias, imprecision, limit of detection (LOD), lower limit of quantification (LLOQ), linearity, carryover, matrix effect (ME), recovery (RE), and dilution integrity were evaluated throughout the method validation process in accordance with suggestions made by the Organization of Scientific Area Committees (OSAC) for Forensic Science, USA [104].

6.2.1 Linearity

Five calibration curves were established on five separate days with 11 calibrators (0.25, 0.5, 1, 2.5, 5, 7.5, 15, 30, 60, 120, 240 ng/mL) for HHC epimers and 7 calibrators (1, 2.5, 5, 10, 25, 50, 100 ng/mL) for HHC metabolites, from the lower (LLOQ) to the upper limit of quantification (ULOQ) calculated by linear least squares regression for each analyte [105]. Calibrators were required to quantify within $\pm 15\%$ of the target concentration ($\pm 20\%$ for LLOQ) and the coefficient of determination had to be higher than or equal to 0.99. Quantifying/confirming transition ratios were required to be within $\pm 20\%$ of the average calibrator transition ion ratio.

6.2.2 Limit of detection and quantification

LOD was tested fortifying 5 different sources of blank blood, urine and oral fluid at the LLOQ and diluting 2, 5, 10, and 20-fold with blank matrix. For each analyte, the LOD was defined as the lowest concentration at which a peak eluted within ± 0.1 min of the average calibrator retention time with a signal/noise ratio higher than or equal to 3 for both transitions and quantifying/confirming transition ratio within $\pm 20\%$ of the average calibrator ratio.

LLOQ was tested fortifying 5 different sources of blank matrix. For each analyte, the LLOQ retention time had to be within ± 0.1 min of the average calibrator retention time and quantify within $\pm 20\%$ of target concentration. In addition, quantifying/confirming transition ratios were required to be within $\pm 20\%$ of the average calibrator ratio.

6.2.3 Carryover and Interferences

Absence of carryover was verified in triplicate injecting a blank sample fortified with the analytes at 5 times the ULOQ followed by a negative sample. If no peak eluted within ± 0.1 minutes of the average calibrator retention time with a signal-to-noise ratio greater than 3 in negative samples, carryover was insignificant.

Five different blank blood, urine, and oral fluid samples were used to determine matrix interferences. Interferences were negligible if no peak eluted within ± 0.1 min of average calibrator retention time with a signal/noise ratio higher than 3. Additionally, blank matrix was tested for potential drug interferences from external sources. For this, fortified matrix samples were spiked with other cannabinoids: 7-hydroxy cannabidiol (7-OH-CBD), 7-carboxy cannabidiol (7-COOH-CBD), 6 α -hydroxycannabidiol (6 α -OH-CBD), 6 β -Hydroxycannabidiol (6 β -OH-CBD), 11-hydroxy-tetrahydrocannabinol (11-OH-THC), and 11-Nor-9-carboxy- Δ 9-tetrahydrocannabinol (THC-COOH) at 3 different concentrations (10, 50 and 100 ng/mL). No signal/noise ratio greater than 3 at ± 0.1 min of the analytes retention period (which ranged from 4.55 to 6.32 min for i-amylose-3 column and from 3.20 to 5.35 min for Lux-amp column) in the quantitative and qualitative ions was the requirement for acceptability.

6.2.4 Dilution integrity and stability

Dilution integrity was assessed in five replicates fortifying blank blood with analytes at 2 times the ULOQ. Samples were diluted two, five, ten and twenty-fold

in blank samples before analysis and were required to quantify within $\pm 20\%$ of target concentration with a quantifying/confirming transition ratio within $\pm 20\%$ of the average calibrator ratio.

Analyte stability was assessed in all biological matrices at room temperature and at 4°C for 24 h, following 3 freeze/thaw cycles (-20°C), and in the LC reconstitution solvent 24 h after extraction and storage in the autosampler (10°C). Internal standard was added immediately before extraction. Stability was assessed in 4 replicates at QC1, QC2, and QC3 concentrations. Room temperature samples and refrigerated samples were analyzed after 24 h. Analytes were considered stable if observed concentrations were within $\pm 20\%$ of target concentration with a quantifying/confirming transition ratio within $\pm 20\%$ of the average calibrator ratio of target. Processed sample stability was measured by extracting low and high QC samples ($n=3$), combining reconstituted samples, dividing them into different autosampler vials, and immediately analyzing them on the instrument. Vials with extracted samples remained on the autosampler (4°C) and were re-injected after 24 h. Finally, mid-term stability was assessed re-analyzing 3 replicates of at QC1,

QC2, and QC3 concentrations after 1 week after QC samples preparation and storage at -20°C.

6.2.5 Matrix effect and recovery

Strategies for the assessment of matrix effect on HPLC-MS/MS produced by B.K. Matuszewski et al. [106] was used to evaluate matrix effect and recovery with blank blood, urine and oral fluid samples from 5 different sources fortified with the analytes at QC1, QC2, and QC3 concentrations. Three sample sets were prepared, with set pre QC (A) samples fortified with the analytes before extraction, set post QC (B) samples extracted and fortified with the analytes immediately before the evaporation, and set neat (C) standards in LC reconstitution solvent. For each analyte, ion suppression or enhancement was calculated by dividing mean LC-MS/MS peak area of set A by mean analyte peak area of set B. Ion suppression or enhancement was calculated by dividing mean LC-MS/MS peak area of set B by mean analyte peak area of set C, minus 1. Samples were required to quantify within $\pm 20\%$ of target concentration with a quantifying/confirming transition ratio within $\pm 20\%$ of the average calibrator ratio. Accuracy and imprecision were calculated for

each matrix type at the QC concentrations. Acceptable criteria were $\pm 30\%$ of target and 20% CV for accuracy and imprecision, respectively.

6.3 Results

6.3.1 Method development

The aim of this study was to develop an HPLC-MS/MS method for the quantitative determination of 9R-HHC and 9S-HHC epimers and their metabolites. For this reason, four polysaccharide-based chiral columns mentioned in the Experimental part and two achiral columns were tested in methanol and in different mobile phase composed with mobile phase A: 5 mmol/L ammonium formate in water and mobile phase B: Methanol + 0.1% formic acid to separate HHC epimers and their metabolites.

The use of Lux i-Amylose-3 chiral column in combination with methanol in isocratic elution mode accomplished the baseline separation of HHC stereoisomers in all the biological matrices, with retention times of 7.58 and 8.05 for 9R-HHC and 9S-HHC, respectively (Fig. 20).

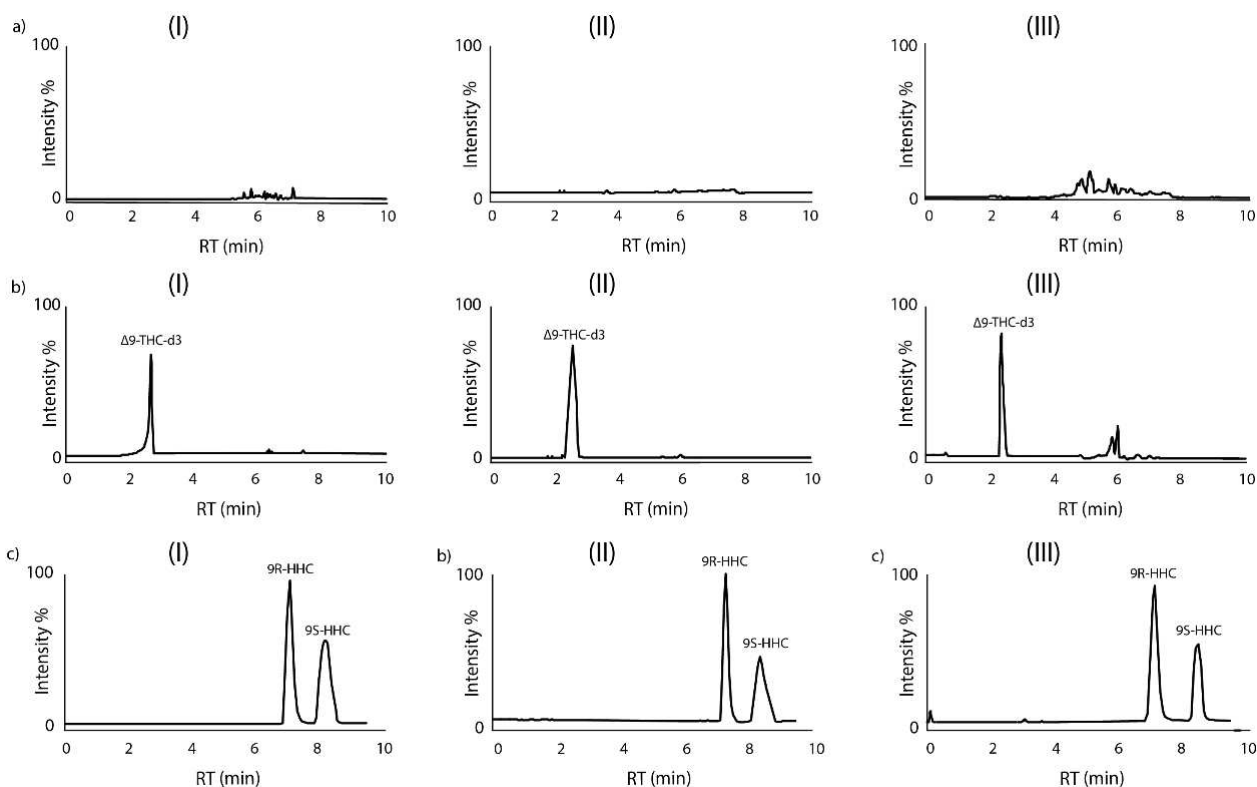


Figure 20: UHPLC-MS/MS chromatograms of blank (a) and negative (b) blood (I), oral fluid (II) and urine (III) samples. Blank blood, oral fluid and urine samples were fortified with a 1:1 mixture of 9R- and 9S-HHC at the limit of quantification (c). Separation of stereoisomers was achieved on Lux i-Amylose-3 column (4.6 x 250 mm, 5 μ m particles). The mobile phase was isocratic with 100% methanol and 0.5 ml/min flow-rate.

In the case of metabolites, the chiral column Lux i-Amylose-3 did not show promising separation of the epimers. It was therefore decided to try again with the Lux AMP column, which in the case of HHC stereoisomers had not shown good peak separation. The chiral columns Lux AMP in combination with methanol and water 80:20 (v/v) isocratic elution showed the best results (Fig. 21). Under these

conditions, six peaks could be detected, as some of them are completely overlapping. As shown in figure 21, separation of 11-OH-9R-HHC and 8S-OH-9S-HHC, as well as separation of 8R-OH-9R-HHC and 11-OH-9S-HHC were impossible. In this case for the identification and quantification of HHC metabolites only multiple-reaction monitoring (MRM) mode was used (Fig. 22).

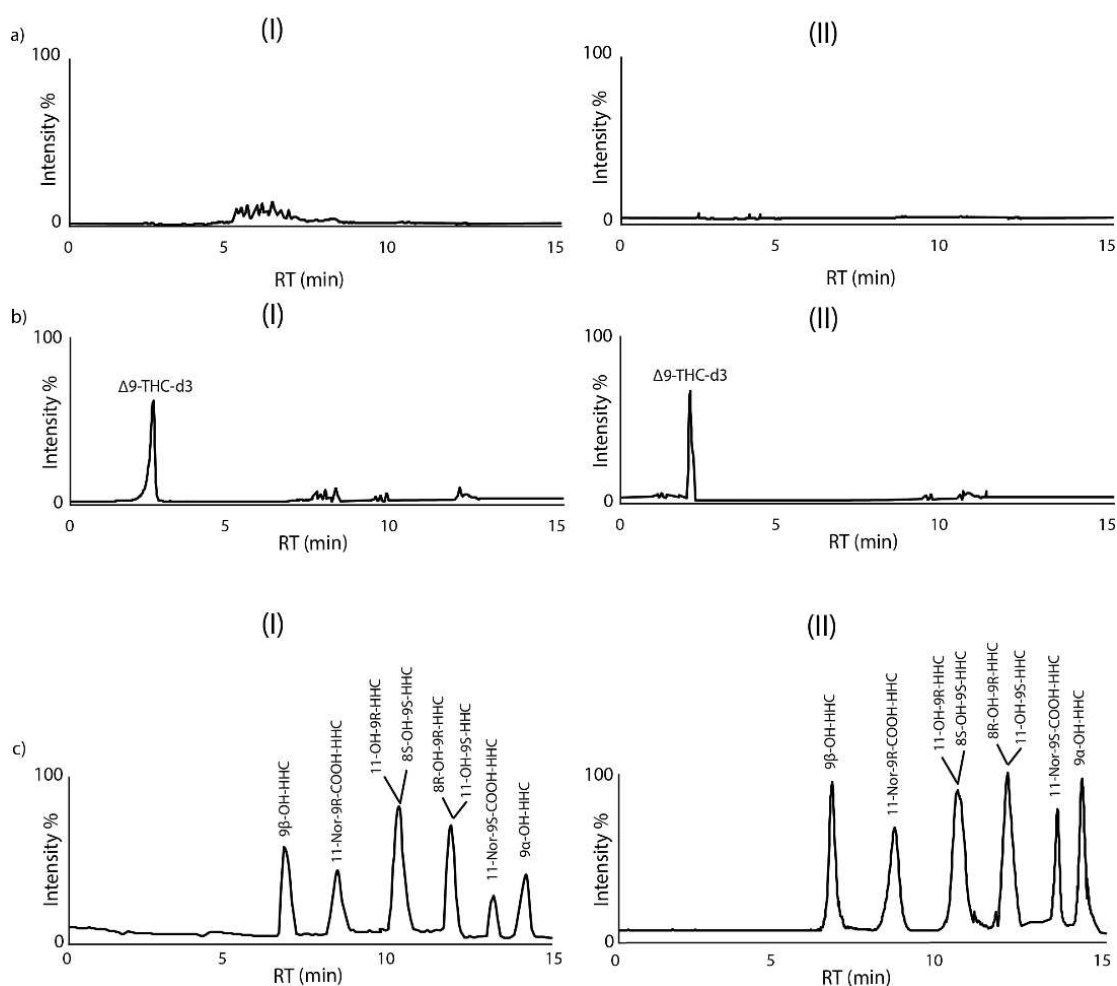


Figure 21: UHPLC-MS/MS chromatograms of blank (a) and negative (b) urine (I) and blood (II) samples, and blank real samples fortified with a 1:1 mixture of HHC metabolites at the limit

of quantification (c). Separation of metabolites was achieved Lux-AMP column (4.6 x 150 mm, 3 μ m particles). The mobile phase was isocratic with 80% methanol and 20% water and flow-rate 0.5 ml/min.

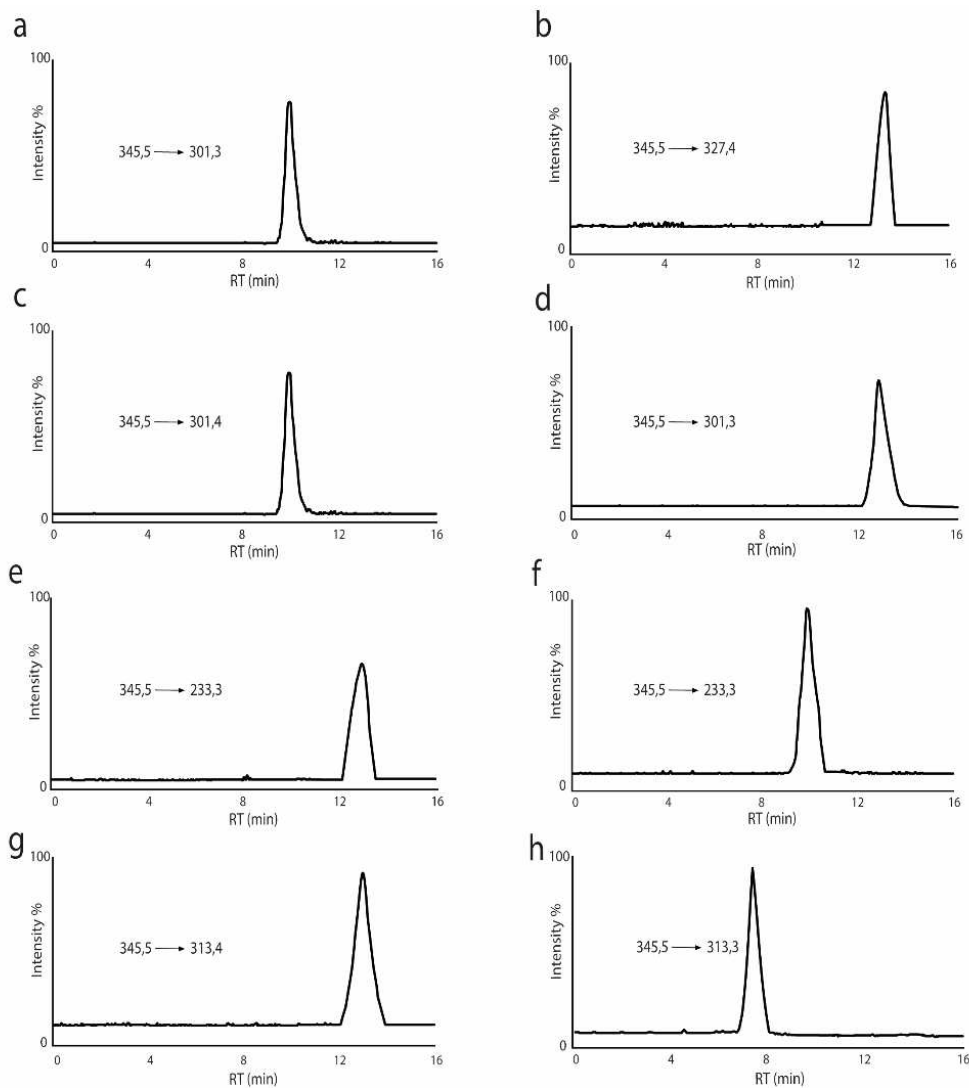


Figure 22: MRM transitions of HHC metabolites in negative ionization mode: a) 11-Nor-9R-COOH-HHC, b) 11-Nor-9S-COOH-HHC, c) 11-OH-9R-HHC, d) 11-OH-9S-HHC, e) 8R-OH-9R-HHC, f) 8S-OH-9S-HHC, g) 9 α -OH-HHC, h) 9 β -OH-HHC

6.3.2 Method validation

The analytical method was fully validated in all the human biological matrices mentioned above, over five consecutive days, following the most recent criteria for bioanalytical method development and validation [17]. The best fit calibration model was a linear least-squares regression model with $1/x^2$ weighting, as confirmed by Mandel test coefficients (p-value and F_{crit} 95 %) [18]. All coefficient of determination results were greater than or equal to 0.99. Validation parameters in human blank whole blood, urine, and oral fluid are reported in Table 4. Separate calibration curves were constructed for HHC stereoisomers in the concentration range of 0.25-240 ng/mL in blood, urine and oral fluid, and 1-100 ng/mL for metabolites in urine, respectively. LOQ was set as the lowest non-zero calibrator for each analyte. Lower limit of quantification (LLOQ) was 0.25 ng/mL in all biological matrices for HHC epimers and 1 for its metabolites. Accuracy and imprecision were calculated at the following three QC concentrations (n = 3): 0.75, 96 and 192 ng/mL for 9R- and 9S-HHC. For HHC metabolites QC concentrations were 3, 40 and 80 ng/mL. Bias was <20% of the target. The ANOVA approach

defined by OSAC guidelines determined the overall within- and between-run imprecision [17]. All CV values were less than 20%, as shown in Table 4. There was no carryover observed with any of the analytes under consideration and there were no interfering peaks in any of the biological matrices analyzed. Dilution integrity was evaluated by extracting blood, urine and oral fluid samples with concentrations two times the ULOQ and diluting the samples 2-, 5-, 10- and 20-fold in blank blood, urine and oral fluid. Concentrations of replicates (n = 5) for the diluted samples were within $\pm 20\%$ of the target for all compounds. The compound stability in blood, urine and oral fluid was evaluated by repeated analysis of five replicates of the three QC samples. All analytes were stable at room temperature, 4 °C, in the autosampler (10°C) and -20 °C for 24 h, after three freeze/thaw cycles, and when stored at -20 °C up to one week after QC sample preparation (concentration differences less than 20% with respect to time zero response), in blood and urine as well as in oral fluid. The method achieved good selectivity and specificity and allows the quantification of 9R-HHC and 9S-HHC and its metabolites, after sample preparation of about 1 hour, using low sample volume (100 μ L). These results demonstrate the applicability of the validated method for

routine analysis in a high-throughput laboratory. Matrix effects were evaluated at low (0.75 ng/mL), mid (96 ng/mL) and high (192 ng/mL) for HHC epimers, and 3, 40 and 80 ng/mL for its metabolites, respectively. Concentrations and the post-extraction addition method determined ionization suppression (negative value) or ionization enhancement (positive value) within $\pm 20\%$ for all analytes, in all the tested biological matrices.

Table 4: Method validation parameters and Mandel’s fitting test (p-value and Fcrit 95%) for analytes under investigation in urine, oral fluid and blood samples.

Abbreviations: LOD, Limit of detection; LOQ, Limit of quantification; L, low quality control; M, medium quality control; H, high quality control; CV, coefficient of variation.

SAMPLE TYPE	ANALYTE	Linear range ng mL ⁻¹	r ²	P-value	F _{crit(95%)}	LOD ng mL ⁻¹	LOQ ng mL ⁻¹	QC ng mL ⁻¹			Accuracy ng mL ⁻¹			Intra-day precision CV (%)			Inter-day precision CV (%)			Recovery (%)			Matrix effect (%)		
								L	M	H	L	M	H	L	M	H	L	M	H	L	M	H	L	M	H
Urine	9R-HHC	0.25-240	0.9983	0.125	0.500	0.1	0.25	96	192	101	98.8	117	103	1.8	1.9	2.9	3.6	3.9	7.1	103	98	96	5.2	-3.2	-6.1
	9S-HHC	0.25-240	0.9996	0.321	0.456	0.1	0.25	96	192	108	105	101	119	2.5	4.0	6.1	3.7	5.9	1.1	102	102	105	7.3	-4.0	-8.5
	11-Nor-9R-COOH-HHC	1-100	0.9995	0.552	0.128	0.5	1	3	40	80	93.0	98.6	113	1.7	3.9	1.7	2.2	4.6	2.2	113	102	103	1.5	-1.8	1.2
	11-Nor-9S-COOH-HHC	1-100	0.9992	0.125	0.046	0.5	1	3	40	80	113	96.7	105	1.4	6.5	3.8	3.3	5.8	3.7	99.1	104	94.2	0.5	2.5	-7.0
	11-OH-9R-HHC	1-100	0.9947	0.032	0.036	0.5	1	3	40	80	110	98.8	117	2.7	6.5	3.8	3.3	5.9	3.9	101	102	96	5.2	-2.1	1.6
	11-OH-9S-HHC	1-100	0.9921	0.249	0.134	0.5	1	3	40	80	102	96.5	101	2.5	4.0	6.1	2.1	7.1	2.2	111	105	107	3.1	-6.0	0.6
	8R-OH-9R-HHC	1-100	0.9953	0.665	0.168	0.5	1	3	40	80	109	113	95.3	2.4	4.1	5.9	1.2	6.7	3.8	106	97.3	113	4.0	5.1	4.7
	8R-OH-9S-HHC	1-100	0.9986	0.741	0.096	0.5	1	3	40	80	108	105	101	1.3	2.1	1.9	3.6	7.1	3.2	103	103	107	3.1	-6.0	0.6
	9α-OH-HHC	1-100	0.9953	0.215	0.0875	0.5	1	3	40	80	120	95.8	117	1.4	3.5	5.0	3.7	5.9	3.9	112	103	96	7.3	-5.2	1.9
	9β-OH-HHC	1-100	0.9923	0.857	0.365	0.5	1	3	40	80	108	106	98.4	3.8	4.6	3.8	7.1	6.5	2.5	107	95.9	98	8.1	2.9	-1.6
Oral Fluid	9R-HHC	0.25-240	0.9983	0.256	0.325	0.1	0.25	96	192	99.2	93.9	112	119	1.9	5.8	0.9	3.0	5.7	2.7	119	102	99.4	-4.0	-2.1	-3.8
	9S-HHC	0.25-240	0.9993	0.152	0.485	0.1	0.25	96	192	105	101	103	2.2	4.6	2.2	6.5	3.8	3.3	112	93.8	107	2.5	4.0	6.1	
	11-Nor-9R-COOH-HHC	2.5-100	0.9998	0.737	0.763	1	2.5	7.5	40	80	107	104	98	5.4	4.0	9.7	0.6	7.1	1.1	109	101	97.4	6.4	2.4	6.1
	11-Nor-9S-COOH-HHC	2.5-100	0.9955	0.514	0.148	1	2.5	7.5	40	80	93.6	93.5	102	3.7	2.5	8.0	2.7	5.5	0.7	106	93.9	98	9.9	1.7	-8.5
	11-OH-9R-HHC	2.5-100	0.9939	0.852	0.047	1	2.5	7.5	40	80	98.7	105	102	7.8	3.7	1.2	0.2	1.2	9.6	107	106	96	1.2	-4.2	1.2
	11-OH-9S-HHC	2.5-100	0.9945	0.366	0.165	1	2.5	7.5	40	80	98.1	114	104	0.5	2.4	6.0	1.9	7.1	0.8	93.8	105	10	9.8	7.9	7.4
	8R-OH-9R-HHC	2.5-100	0.9996	0.037	0.034	1	2.5	7.5	40	80	99.6	103	102	5.6	2.8	1.6	1.6	1.3	9.4	102	114	103	7.4	6.5	1.6
	8R-OH-9S-HHC	2.5-100	0.9987	0.492	0.068	1	2.5	7.5	40	80	104	109	97.3	3.1	6.7	0.6	8.1	0.6	1.4	106.1	94.1	94.1	9.0	3.4	0.1
	9α-OH-HHC	2.5-100	0.9983	0.785	0.096	1	2.5	7.5	40	80	105	112	103	4.3	5.1	1.5	6.0	4.8	0.9	115	99.8	96.8	4.7	-4.0	7.5
	9β-OH-HHC	2.5-100	0.9993	0.241	0.597	1	2.5	7.5	40	80	106	92.9	103	8.4	2.9	8.5	3.4	0.6	8.3	110	93.5	106	8.3	4.4	0.6

6.4 Application to human samples

To demonstrate the suitability of the method developed in authentic cases, the validated approach was subsequently applied to real samples. Blood, urine and oral fluid specimens were collected from 2 healthy male volunteers (33 and 35 years old) after administration of controlled doses (25 mg) of 9R-HHC and 9S-HHC mixture by inhalation. The equal content of both HHC epimers in the administered mixture was proved by HPLC analysis of the material on Lux i-Amylose-3 column (Fig. 23). Although the behavior of the selected chiral columns (Lux i-Amylose-3 and Lux AMP) is quite complementary, neither was able to resolve all stereoisomer pairs in a single chromatographic separation. Therefore, it was decided to study the separation of HHC epimers and the epimers of their metabolites in real samples using two alternative chiral columns. For chromatograms of separation HHC epimers and its metabolites in real human samples, see Figure 24. The concentrations for 9R-HHC and 9S-HHC in blood were 2.5-68.4 and 2.2-26.1 ng/mL, respectively. In case of urine the concentration was 2.8-11.2 for 9R- and 2.1-20.6 ng/mL 9S-HHC, respectively.

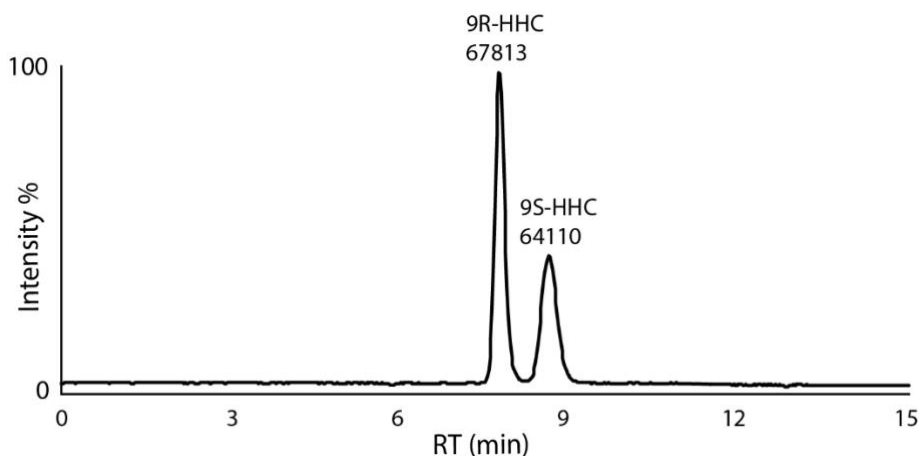


Figure 23: separation of HHC epimers, extracted from the mixture of HHC resin and tobacco on Lux i-Amylose-3 column. For separation conditions see the legends to figure 20.

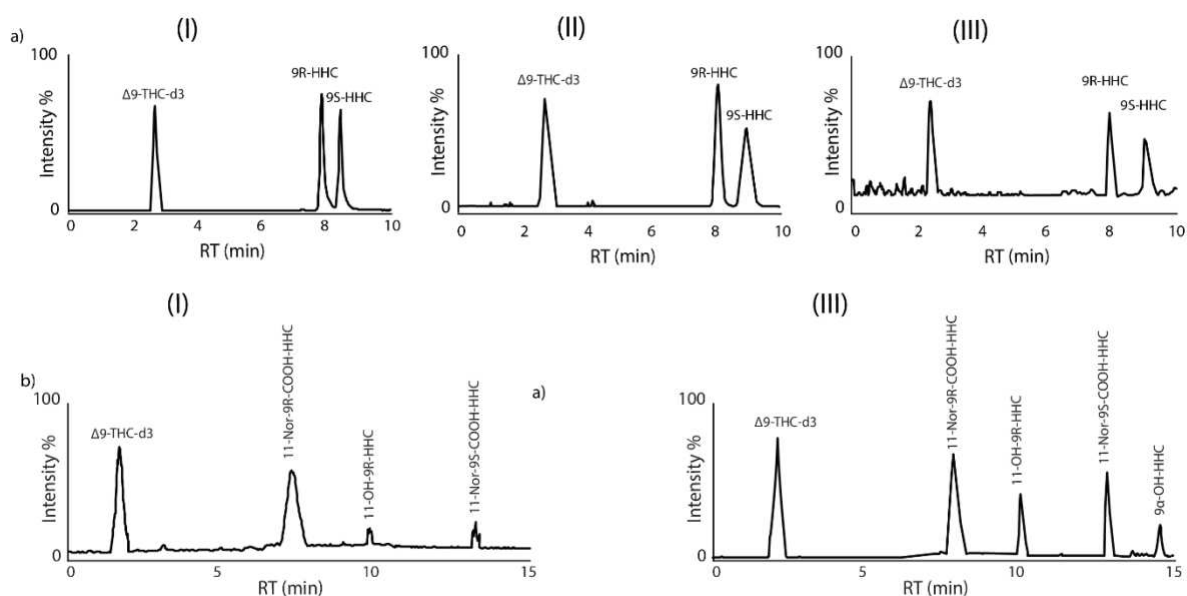


Figure 24: chromatogram of separation HHC epimers (a) and its metabolites (b) in human real urine (I), oral fluid (II) and blood (III) samples. For separation conditions see the legends to figures 20 and 21.

In oral fluid samples average concentration range was 0.5-228.2 and 2.1-120.4 ng/mL for 9R- and 9S-HHC, respectively.

In the case of HHC metabolites only four metabolites were detected and quantified in urine samples. The detected metabolites were 11-Nor-9R-COOH-HHC, 11-Nor-9S-COOH-HHC, 11-OH-9R-HHC and 9 α -OH-HHC, with 11-Nor-9R-COOH-HHC representing the most abundant metabolite (22.09 ng/mL) and 9 α -OH-HHC as metabolite with the lowest concentration (2.58 ng/mL). For other metabolites (11-Nor-9S-COOH-HHC and 11-OH-9R-HHC) the maximum concentrations were 5.68 ng/mL and 4.16 ng/mL, respectively.

Three metabolites were detected in blood real samples (11-Nor-9R-COOH-HHC, 11-Nor-9S-COOH-HHC and 11-OH-9R-HHC), from these three metabolites concentration of 11-Nor-9S-COOH-HHC and 11-OH-9R-HHC were negligible (less than LLOQ). Maximum concentration for 11-Nor-9R-COOH-HHC was 11.6 ng/mL. 8-OH-metabolites of HHC were not detected in any of the biological fluids studied.

7. IN VIVO METABOLISM

7.1 Methods

Blood, urine, and oral fluid samples were obtained from 7 healthy volunteers who were invited to participate in the clinical study through word of mouth. Eligibility criteria included being of legal age, no consumption of HHC in the preceding 6 months, passing a general physical examination, routine laboratory analysis, and electrocardiogram. All subjects provided written informed consent, and the study was conducted in accordance with the Declaration of Helsinki and approved by the Institutional Ethics Committee (IRCCS-INRCA Ancona). Subjects participated in a 48-hour experimental session, with the initial 10 hours conducted on an outpatient basis at the Patient Care and Scientific Research Institute (IRCCS-INRCA) in Ancona. The facility was equipped for clinical studies and had an open balcony where subjects could smoke *ad libitum*.

Before the study commenced, a pharmacological screening of urine was performed for all volunteers using the Dionex UltiMate 3000 chromatographic system coupled with a Thermo Scientific Q Exactive LC-HRMS/MS mass

spectrometer. The screening results were negative for common drug abuse substances (opioids, cocaine, cannabinoids, and amphetamines).

Seven volunteers participated in the study, including 4 males (subjects 1, 2, 3, 5) and 3 females (subjects 4, 6, 7), with an average age of 37 years (± 16.1) and an average body weight of 70 kg (± 10) for males and 60 kg (± 5) for females. Subjects 4, 5, and 6 reported a smoking habit.

Each participant smoked a cigarette containing 25 mg of HHC mixed with 500 mg of tobacco. A 21-gauge venous access was established by the dedicated nursing service in the antecubital vein (cephalic or basilic vein) for the entire outpatient phase to collect blood samples. Two physicians were present for assistance in case of adverse reactions.

Biological samples were collected at time zero, before HHC inhalation, and subsequently. Blood samples were collected at time zero and at 10', 20', 30', 1, 2, and 3 hours after consumption. Urine samples were collected at time zero and at 10', 20', 30', 1, 2, 3, 6, 12, 24, and 48 hours after administration. Oral fluid samples were collected before intake and at 10', 20', 30', 45', 1, 1.5, 2, and 3 hours after administration. In total, 168 biological samples were collected.

Measurements started in the late afternoon (between 5:45 and 7:15 PM). Participants were free to report any symptoms experienced during the entire experimentation. In the initial study phase, as later described in detail, blood pressure, heart rate, oxygen saturation, and body temperature were measured.

For 6 subjects, blood samples were collected at time zero and at 10', 20', 30', 1, 2, and 3 hours after consumption, while in a single case, the study was terminated after the first four collections (at time zero, 10', 20', and 30'). Regarding urine samples, it was possible to collect samples at 30', 1, 2, 3, 6, 12, 24, and 48 hours for only 3 subjects, for 3 subjects at 10', 30', 1, and 2 hours, while in one case, no sample could be collected due to study discontinuation. Regarding oral fluid samples, all planned samples were collected in 6 cases, while in a single case, only the first sample at 10' after administration could be collected.

7.2 Data Analysis and Results

All data related to the obtained results are reported; data on the concentrations of HHC and metabolites in the examined matrices for the subject who had to

discontinue the study (subject 7) are not reported. Data regarding the clinical symptoms presented by the same subject will be presented later.

The intervals of average concentrations in the blood were 6.84-30.02 ng/mL for 9R-HHC (with the lowest average concentration observed in the measurements at 3 hours after intake and the highest average concentration observed at the measurement taken at 20 minutes after administration) and 6.69-13.03 ng/mL for 9S-HHC (with the lowest average concentration observed in the measurements at 3 hours after intake and the highest average concentration at the measurement taken at 20 minutes after administration).

In oral fluid samples, the average concentration range was 1.33-129.35 ng/mL for 9R-HHC and 9.4-99.25 ng/mL for 9S-HHC. Regarding 9R-HHC, the lowest average concentration was observed in measurements taken 3 hours after HHC intake, and the highest concentration was observed at measurements taken at 20 minutes. For 9S-HHC, the lowest average concentration was still observed in measurements taken at 3 hours, while the highest average concentration was found in measurements taken at 10 minutes after HHC administration.

Regarding measurements on urine samples, the average concentration ranged from 3.07-8.88 ng/mL for 9R-HHC (with the lowest average concentration observed in measurements taken at 48 hours and the peak urinary concentration observed at 6 hours after intake) and 2.46-14.7 ng/mL for 9S-HHC (with the lowest average concentration observed in measurements taken at 48 hours and the peak urinary concentration observed at 3 hours after intake).

Three metabolites were detected in blood samples (11-Nor-9R-COOH-HHC, 11-Nor-9S-COOH-HHC, and 11-OH-9R-HHC); the concentrations of the metabolites 11-Nor-9S-COOH-HHC and 11-OH-9R-HHC were negligible (below the LLOQ). 11-NOR-9R-COOH-HHC was detected and quantified in plasma samples from two enrolled subjects with values of 11.66 ng/mL (peak plasma at 30 minutes) and 6.32 ng/mL (peak plasma at 1 hour); in both cases, the minimum plasma concentration was observed at 10 minutes with values of 0.80 and 0.10 ng/mL, respectively.

The metabolites detected in urine were 11-NOR-9R-COOH-HHC (4.9-21.53), 11-NOR-9S-COOH-HHC (1.16-5.08), 11-OH-9R-HHC (0.57-3.91), and 9 α -OH-HHC (0.81-2.69). The minimum urinary concentrations of the metabolites 11-

NOR-9R-COOH-HHC, 11-NOR-9S-COOH-HHC, and 9 α -OH-HHC were observed in measurements taken at the end of the experimental session (48 hours after intake), while the highest average concentration values were observed at 6 hours after HHC intake. Regarding the metabolite 11-OH-9R-HHC, the highest average concentration was observed at 3 hours after intake, while the lowest average concentration was in urine collected at the end of the 48 hours stipulated by the study.

11-NOR-9R-COOH-HHC represented the most abundant metabolite, and 9 α -OH-HHC as the metabolite with the lowest concentration. The 8-OH metabolites of HHC were not detected in any of the studied biological fluids.

Table 5 shows the plasma concentrations of 9R-HHC (ng/mL) at each time interval in which the sample was collected and analyzed. The peak plasma concentration is reached approximately 20 minutes after intake.

Table 5: Plasma concentrations of 9R-HHC observed at various time intervals after HHC administration in ng/mL.

Time	Subj. 1	Subj. 2	Subj. 3	Subj. 4	Subj. 5	Subj. 6	Average	SD	SE
0	0.00	0.00	0.00	0.00	0.00	0.00	0.00	0.00	0.00
10'	13.68	3.92	5.00	94.95	13.70	15.45	24.45	34.88	24.66
20'	14.59	4.13	6.68	118.37	18.53	17.81	30.02	43.68	30.89
30'	19.39	3.77	4.05	73.23	19.46	19.27	23.19	25.66	18.14
1 h	9.62	3.66	3.43	21.04	10.74	56.11	17.43	20.00	14.14
2 h	5.09	3.53	2.94	13.26	6.23	27.78	9.81	9.55	6.76
3 h	4.42	3.49	2.89	12.43	4.64	13.18	6.84	4.67	3.30
KE	0.34	0.03	0.15	0.77	0.36	0.32	0.33	0.25	0.18
T ½ h	17.79	178.07	40.95	7.79	16.45	18.53	46.60	65.34	46.20
AUC h× ng/mL	26.06	10.71	10.09	87.99	28.69	93.09	42.77	37.82	26.74
Clast	4.42	3.49	2.89	12.43	4.64	13.18	6.84	4.67	3.30
Cmax	19.39	4.13	6.68	118.37	19.46	56.11	37.36	43.82	30.99
Tmax	0.30	0.20	0.20	0.20	0.30	1.00	0.37	0.31	0.22

In Table 6, the plasma concentrations of 9S-HHC (ng/mL) found at each time interval when the sample was collected and analyzed are reported. The peak plasma concentration is reached approximately 20 minutes after intake.

Table 6: Plasma concentrations of 9S-HHC found at different time intervals after the administration of HHC in ng/mL.

Time	Subj. 1	Subj. 2	Subj. 3	Subj. 4	Subj. 5	Subj. 6	Average	SD	SE
0	0.00	0.00	0.00	0.00	0.00	0.00	0.00	0.00	0.00
10'	7.75	2.83	4.07	35.70	8.34	9.08	11.30	12.21	8.63
20'	9.03	3.07	4.46	42.50	9.85	9.29	13.03	14.71	10.40
30'	10.36	4.37	4.16	33.03	9.60	10.13	11.94	10.71	7.57

1 h	22.91	3.22	3.80	14.21	6.63	14.96	10.95	7.74	5.47
2 h	18.72	2.41	3.71	9.88	4.20	20.02	9.82	7.84	5.54
3 h	5.12	2.30	3.08	8.15	4.39	17.10	6.69	5.49	3.88
KE	0.56	0.15	0.13	0.61	0.34	0.07	0.31	0.23	0.16
T ½ h	10.65	40.88	45.79	9.87	17.64	87.82	35.44	29.89	21.13
AUC h× ng/mL	46.57	8.63	11.00	47.06	17.69	47.18	29.69	19.13	13.53
Clast	5.12	2.30	3.08	8.15	4.39	17.10	6.69	5.49	3.88
Cmax	22.91	4.37	4.46	42.50	9.85	20.02	13.03	14.57	10.30
Tmax	1.00	0.30	0.20	0.20	0.20	2.00	0.65	0.73	0.52

In Table 7, the plasma concentrations of 11-NOR-9R- COOH-HHC (ng/mL) found at each time interval when the sample was collected and analyzed are reported. The peak plasma concentration is reached approximately 30 minutes after smoking.

Table 7: Plasma concentrations of 11-NOR-9R-COOH-HHC found at different time intervals after the administration of HHC in ng/mL.

Time	Subj. 1	Subj. 2	Subj. 3	Subj. 4	Subj. 5	Subj. 6	Average	SD	SE
0	0.00	0.00	0.00	0.00	0.00	0.00	0.00	0.00	0.00
10'	0.00	0.00	0.00	0.80	0.00	0.10	0.16	0.36	0.25
20'	0.00	0.00	0.00	6.33	0.00	2.00	1.27	2.83	2.00
30'	0.00	0.00	0.00	11.66	0.00	5.24	2.33	5.21	3.69
1 h	0.00	0.00	0.00	5.71	0.00	6.32	1.14	2.55	1.81
2 h	0.00	0.00	0.00	4.79	0.00	3.30	0.96	2.14	1.51
3 h	0.00	0.00	0.00	0.88	0.00	0.90	0.18	0.39	0.28
KE	0.00	0.00	0.00	0.81	0.00	0.56	0.69	0.18	0.13
T ½ h	0.00	0.00	0.00	7.37	0.00	10.63	9.00	2.31	1.63
AUC h×	0.00	0.00	0.00	15.46	0.00	11.43	13.44	2.85	2.01

ng/mL									
Clast	0.00	0.00	0.00	0.88	0.00	0.90	0.89	0.02	0.01
Cmax	0.00	0.00	0.00	11.66	0.00	6.32	8.99	3.77	2.67
Tmax	0.00	0.00	0.00	0.30	0.00	1.00	0.65	0.65	0.46

In Table 8, the concentrations in oral fluid of 9R-HHC (ng/mL) found at each time interval when the sample was collected and analyzed are reported. The peak concentration in oral fluid is reached approximately 20 minutes after intake.

Table 8: Concentrations in oral fluid of 9R-HHC found at different time intervals after the administration of HHC in ng/mL.

Time	Subj. 1	Subj. 2	Subj. 3	Subj. 4	Subj. 5	Subj. 6	Average	SD	SE
0	0.00	0.00	0.00	0.00	0.00	0.00	0.00	0.00	0.00
10'	5.12	51.46	141.31	2.67	88.85	57.93	57.89	52.52	37.14
20'	28.74	164.06	57.24	5.39	451.11	69.56	129.35	166.73	117.90
30'	9.97	60.96	35.92	14.04	206.41	58.42	64.29	72.84	51.50
45'	9.90	45.63	26.42	20.80	64.30	43.35	35.07	19.73	13.95
1 h	6.45	33.58	13.36	16.25	3.06	42.50	19.20	15.59	11.03
1.5 h	3.59	32.74	1.26	13.07	1.87	9.44	10.33	11.91	8.42
2 h	2.07	13.31	1.04	6.46	1.03	1.16	4.18	4.94	3.49
3 h	1.63	4.42	0.56	0.20	0.88	0.27	1.33	1.60	1.13
KE	0.78	1.14	1.81	1.90	2.37	2.34	1.72	0.64	0.45
T ½ h	7.65	5.26	3.32	3.15	2.53	2.57	4.08	2.02	1.43
AUC h× ng/mL	14.95	86.74	34.00	28.74	101.41	56.23	53.68	34.31	24.26
Clast	1.63	4.42	0.56	0.20	0.88	0.27	1.33	1.60	1.13
Cmax	28.74	164.06	141.31	20.80	451.11	69.56	145.93	160.44	113.45
Tmax	0.20	0.20	0.10	0.45	0.20	0.20	0.23	0.12	0.08

In Table 9, the concentrations in oral fluid of 9S-HHC (ng/mL) found at each time interval when the sample was collected and analyzed are reported.

Table 9: Concentrations in oral fluid of 9S-HHC found at different time intervals after the administration of HHC in ng/mL.

Time	Subj. 1	Subj. 2	Subj. 3	Subj. 4	Subj. 5	Subj. 6	Average	SD	SE
0	0.00	0,00	0,00	0,00	0,00	0,00	0,00	0,00	0,00
10'	13.45	355.62	10.46	13.71	145.04	57.21	99.25	135.76	96.00
20'	46.91	57.45	71.37	21.40	219.60	100.71	86.24	70.42	49.80
30'	33.55	43.47	67.05	23.04	136.63	60.77	60.75	40.64	28.74
45'	30.72	29.34	51.91	33.41	79.51	35.69	43.43	19.46	13.76
1 h	29.99	27.95	27.73	67.58	64.15	24.79	40.37	19.85	14.04
1.5 h	27.20	16.42	12.80	34.46	20.39	24.48	22.62	7.80	5.52
2 h	26.08	5.90	4.55	32.59	3.77	18.79	15.28	12.37	8.74
3 h	14.90	1.06	2.45	28.13	1.98	7.87	9.40	10.55	7.46
KE	0.35	1.61	1.44	0.09	1.84	0.89	1.04	0.71	0.50
T ½ h	17.02	3.72	4.18	68.04	3.26	6.76	17.16	25.45	18.00
AUC h× ng/mL	76.27	64.86	57.49	105.12	115.77	75.70	82.54	22.98	16.25
Clast	14.90	1.06	2.45	28.13	1.98	7.87	9.40	10.55	7.46
Cmax	46.91	355.62	71.37	67.58	219.60	100.71	143.63	120.76	85.39
Tmax	0.20	0.10	0.20	1.00	0.20	0.20	0.32	0.34	0.24

In Table 10, the urinary concentrations of 9R-HHC (ng/mL) found at each time interval when the sample was collected and analyzed are reported.

Table 10: Urinary concentrations of 9R-HHC found at different time intervals after the administration of HHC in ng/mL.

Time	Subj. 1	Subj. 2	Subj. 3	Subj. 4	Subj. 5	Subj. 6	Average	SD	SE
-------------	----------------	----------------	----------------	----------------	----------------	----------------	----------------	-----------	-----------

0	0.00	0.00	0.00	0.00	0.00	0.00	0.00	0.00	0.00
30'	3.43	3.80	4.04	3.49	4.19	3.88	3.79	0.33	0.24
1	4.57	4.25	5.49	4.29	4.49	4.39	4.62	0.51	0.36
2	5.76	5.13	9.34	7.35	5.39	6.24	6.59	1.76	1.24
3	6.79	6.84	10.42	7.65	8.96	9.26	8.13	1.55	1.09
6	7.59	9.67	7.65	9.88	9.61	10.88	8.88	1.15	0.82
12	4.34	9.80	6.88	6.43	11.23	11.22	7.73	2.76	1.95
24	3.08	8.73	4.64	4.79	3.54	7.05	4.96	2.23	1.58
48	2.70	3.40	3.49	2.59	3.16	4.22	3.07	0.41	0.29
KE	0.21	0.41	0.34	0.40	0.05	0.22	0.27	0.14	0.10
T ½ h	29.20	14.65	17.60	15.17	120.14	26.93	37.28	41.05	29.03
AUC h× ng/mL	185.49	353.32	258.09	247.18	274.53	357.37	279.33	66.15	46.77
Clast	2.70	3.40	3.49	2.59	3.16	4.22	3.26	0.60	0.42
Cmax	7.59	9.80	10.42	9.88	11.23	11.22	10.02	1.34	0.95
Tmax	6.00	12.00	3.00	6.00	12.00	12.00	8.50	3.99	2.82

In Table 11, the urinary concentrations of 9S-HHC (ng/mL) found at each time interval when the sample was collected and analyzed are reported.

Table 11: Urinary concentrations of 9S-HHC found at different time intervals after the administration of HHC in ng/mL.

Time	Subj. 1	Subj. 2	Subj. 3	Subj. 4	Subj. 5	Subj. 6	Average	SD	SE
0	0.00	0.00	0.00	0.00	0.00	0.00	0.00	0.00	0.00
30'	2.31	2.27	2.36	2.30	8.56	5.15	3.56	2.79	1.98
1 h	2.90	3.25	4.05	5.36	11.59	10.40	5.43	3.57	2.52
2 h	4.35	8.06	8.37	7.32	16.34	12.98	8.89	4.46	3.15
3 h	8.30	10.33	10.35	8.36	33.00	16.59	14.07	10.63	7.52
6 h	5.43	8.23	7.69	10.34	17.01	12.46	9.74	4.42	3.13
12 h	4.54	5.59	5.31	2.35	12.11	8.68	5.98	3.65	2.58
24 h	3.80	4.63	3.35	2.32	8.16	3.59	4.45	2.23	1.58

48	2.36	2.88	2.90	1.78	2.39	2.40	2.46	0.46	0.32
KE	0.36	0.46	0.42	0.12	0.85	0.72	0.49	0.26	0.18
T ½ h	16.57	13.17	14.18	49.83	7.04	8.38	18.19	15.91	11.25
AUC h× ng/mL	186.27	237.49	210.84	160.30	456.14	284.38	255.90	107.02	75.67
Clast	2.36	2.88	2.90	1.78	2.39	2.40	2.45	0.41	0.29
Cmax	8.30	10.33	10.35	10.34	33.00	16.59	14.82	9.34	6.61
Tmax	3.00	3.00	3.00	6.00	3.00	3.00	3.50	1.22	0.87

In Table 12, the urinary concentrations of 11-NOR-9R-COOH-HHC (ng/mL) found at each time interval when the sample was collected and analyzed are reported.

Table 12: Urinary concentrations of 11-NOR-9R-COOH-HHC found at different time intervals after the administration of HHC in ng/mL.

Time	Subj. 1	Subj. 2	Subj. 3	Subj. 4	Subj. 5	Subj. 6	Average	SD	SE
0	0.00	0.00	0.00	0.00	0.00	0.00	0.00	0.00	0.00
30'	7.24	4.86	4.04	6.22	7.11	6.20	5.89	1.40	0.99
1 h	10.02	14.19	7.22	9.25	11.19	8.24	10.37	2.58	1.82
2 h	12.07	19.21	9.32	11.40	13.31	11.29	13.06	3.73	2.64
3 h	25.05	14.55	12.57	16.35	19.42	14.46	17.59	4.87	3.45
6 h	37.42	6.31	19.72	22.22	21.96	22.51	21.53	11.05	7.81
12 h	23.44	5.04	15.13	19.03	15.32	18.43	15.59	6.80	4.81
24 h	16.24	4.30	13.04	13.70	11.17	5.32	11.69	4.51	3.19
48 h	3.45	3.84	6.02	5.11	6.10	3.11	4.90	1.22	0.86
KE	0.83	0.58	0.40	0.57	0.40	0.77	0.59	0.18	0.13
T ½ h	7.21	10.37	14.99	10.51	15.00	7.77	10.97	3.39	2.40
AUC h× ng/mL	786.30	259.33	573.90	633.27	575.21	449.70	546.28	178.01	125.88

Clast	3.45	3.84	6.02	5.11	6.10	3.11	4.61	1.32	0.93
Cmax	37.42	19.21	19.72	22.22	21.96	22.51	23.84	6.79	4.80
Tmax	6.00	2.00	6.00	6.00	6.00	6.00	5.33	1.63	1.15

In Table 13, the urinary concentrations of 11-NOR-9S-COOH-HHC (ng/mL) found at each time interval when the sample was collected and analyzed are reported.

Table 13: Urinary concentrations of 11-NOR-9S-COOH-HHC found at different time intervals after the administration of HHC in ng/mL.

Time	Subj. 1	Subj. 2	Subj. 3	Subj. 4	Subj. 5	Subj. 6	Average	SD	SE
0	0.00	0.00	0.00	0.00	0.00	0.00	0.00	0.00	0.00
30'	1.21	0.55	2.41	1.60	0.77	3.41	1.31	0.74	0.52
1 h	2.28	0.88	4.39	2.49	0.84	4.83	2.18	1.46	1.03
2 h	2.58	1.25	6.47	2.75	1.17	6.49	2.85	2.16	1.52
3 h	2.78	2.08	7.19	3.46	4.18	7.75	3.94	1.98	1.40
6 h	4.84	4.57	7.95	2.33	5.72	10.87	5.08	2.03	1.44
12 h	3.58	2.41	6.29	2.06	4.78	6.39	3.82	1.75	1.23
24 h	2.96	1.83	3.13	1.41	2.27	2.57	2.32	0.73	0.52
48 h	0.64	0.49	2.57	0.83	1.27	1.01	1.16	0.84	0.60
KE	0.75	0.69	0.39	0.45	0.57	0.80	0.61	0.17	0.12
T ½ h	8.00	8.67	15.46	13.46	10.44	7.50	10.59	3.22	2.28
AUC h× ng/mL	125.52	87.50	205.03	76.72	135.45	192.09	137.05	52.69	37.26
Clast	0.64	0.49	2.57	0.83	1.27	1.01	1.14	0.76	0.53
Cmax	4.84	4.57	7.95	3.46	5.72	10.87	6.23	2.72	1.93
Tmax	6.00	6.00	6.00	3.00	6.00	6.00	5.50	1.22	0.87

In Table 14, the urinary concentrations of 11-OH-9R-HHC (ng/mL) found at each time interval when the sample was collected and analyzed are reported.

Table 14: Urinary concentrations of 11-OH-9R-HHC found at different time intervals after the administration of HHC in ng/mL.

Time	Subj. 1	Subj. 2	Subj. 3	Subj. 4	Subj. 5	Subj. 6	Average	SD	SE
0	0.00	0.00	0.00	0.00	0.00	0.00	0.00	0.00	0.00
30'	2.09	2.00	0.95	0.95	2.28	1.04	1.66	0.65	0.46
1 h	3.03	3.06	1.14	1.12	2.45	2.81	2.16	0.97	0.69
2 h	5.04	3.08	2.04	2.47	3.49	8.40	3.22	1.16	0.82
3 h	4.02	4.08	3.10	4.33	4.00	5.10	3.91	0.47	0.33
6 h	3.24	5.09	2.65	3.05	2.16	2.95	3.24	1.11	0.79
12 h	3.06	2.09	1.95	2.06	1.76	2.04	2.18	0.51	0.36
24 h	1.09	1.24	1.14	2.09	1.12	1.03	1.34	0.42	0.30
48 h	0.70	0.06	0.26	0.72	1.09	0.54	0.57	0.41	0.29
KE	0.76	1.54	1.01	0.63	0.30	0.74	0.83	0.42	0.29
T ½ h	7.90	3.91	5.95	9.56	20.12	8.14	9.26	5.67	4.01
AUC h× ng/mL	86.51	79.43	62.71	90.80	73.19	78.07	78.45	9.94	7.03
Clast	0.70	0.06	0.26	0.72	1.09	0.54	0.56	0.36	0.26
Cmax	5.04	5.09	3.10	4.33	4.00	8.40	4.99	1.83	1.29
Tmax	2.00	6.00	3.00	3.00	3.00	2.00	3.17	1.47	1.04

In Table 15, the urinary concentrations of 9 α -OH-HHC (ng/mL) found at each time interval when the sample was collected and analyzed are reported.

Table 15: Urinary concentrations of 9 α -OH-HHC found at different time intervals after the administration of HHC in ng/mL.

Time	Subj. 1	Subj. 2	Subj. 3	Subj. 4	Subj. 5	Subj. 6	Average	SD	SE
0	0.00	0.00	0.00	0.00	0.00	0.00	0.00	0.00	0.00
30'	0.98	1.06	0.20	0.86	0.96	0.61	0.81	0.35	0.25
1 h	1.08	1.33	0.71	0.90	1.16	0.94	1.04	0.24	0.17
2 h	1.45	2.48	0.97	1.12	1.24	1.18	1.45	0.60	0.43
3 h	2.04	3.52	1.46	1.67	2.05	2.12	2.15	0.81	0.57
6 h	3.07	3.11	2.09	2.09	3.07	2.25	2.69	0.54	0.38
12 h	2.05	2.11	1.96	1.11	2.08	1.27	1.86	0.42	0.30
24 h	1.07	0.94	1.56	1.07	1.46	1.07	1.22	0.27	0.19
48 h	0.98	0.60	1.14	0.51	0.83	0.65	0.81	0.26	0.18
KE	0.32	0.71	0.24	0.34	0.40	0.29	0.38	0.17	0.12
T ½ h	18.86	8.40	25.38	17.79	14.98	20.76	17.70	5.72	4.04
AUC h× ng/mL	70.03	68.18	73.33	50.23	75.37	55.13	65.38	1027	7.26
Clast	0.98	0.60	1.14	0.51	0.83	0.65	0.78	0.24	0.17
Cmax	3.07	3.52	2.09	2.09	3.07	2.25	2.68	0.61	0.43
Tmax	6.00	3.00	6.00	6.00	6.00	6.00	5.50	1.22	0.87

7.3 Clinical evidence of in vivo administration of HHC

Simultaneously with the collection of biological matrices, various clinical parameters were monitored in the first 6 hours of observation: blood pressure, heart rate, oxygen saturation, and body temperature. In addition, participants reported subjective symptoms both during the 10 hours of ambulatory observation and subsequently, for a maximum of 48 hours from HHC intake.

Table 16 reports the values of blood pressure (systolic/diastolic mmHg) at different time intervals after the administration of HHC.

Table 16: values of blood pressure (systolic/diastolic mmHg) at different time intervals after the administration of HHC

Diastolic and systolic blood pressure (mmHg)							
Time	Subj. 1	Subj. 2	Subj. 3	Subj. 4	Subj. 5	Subj. 6	Average
0	125/80	110/70	117/75	115/88	100/75	128/85	120/86
10'	125/85	113/77	120/78	98/60	105/80	125/86	90/75
20'	128/84	120/80	130/85	80/55	110/80	127/84	78/40
30'	140/90	123/78	130/82	85/65	115/83	120/82	/
1 h	135/88	115/75	125/80	100/72	115/78	100/70	/
3 h	135/80	115/72	115/82	110/75	110/75	110/80	/
6 h	127/77	110/75	115/85	110/78	108/74	120/84	/

Table 17 reports the values of heart rate (beats per minute) at different time intervals after the administration of HHC.

Table 17: heart rate (beats per minute) at different time intervals after the administration of HHC.

Heart rate (bpm)							
Time	Subj. 1	Subj. 2	Subj. 3	Subj. 4	Subj. 5	Subj. 6	Average
0	59	63	71	69	72	65	62
10'	65	68	73	79	71	69	85
20'	71	70	75	98	82	78	104
30'	78	71	82	97	75	88	/
1 h	65	66	68	78	72	92	/
3 h	65	65	71	70	68	80	/
6 h	62	67	67	72	70	75	/

Table 18 reports the values of oxygen saturation (SpO2 %) at different time intervals after the administration of HHC: time 0, 10', 20', 30', 1, 3, 6 h.

Table 18: oxygen saturation (SpO₂ %) at different time intervals after the administration of HHC

Oxygen saturation level (SpO ₂ %)							
Time	Subj. 1	Subj. 2	Subj. 3	Subj. 4	Subj. 5	Subj. 6	Average
0	99	98	98	99	97	99	97
10'	99	97	99	98	97	99	97
20'	97	99	98	99	98	99	96
30'	98	99	97	98	97	98	/
1 h	99	98	99	98	97	98	/
3 h	98	99	99	99	98	99	/
6 h	98	99	98	98	98	99	/

Table 19 reports the values of body temperature at different time intervals after the administration of HHC.

Table 19: values of body temperature at different time intervals after the administration of HHC.

Body temperature (°C)							
Time	Subj. 1	Subj. 2	Subj. 3	Subj. 4	Subj. 5	Subj. 6	Average
0	36.3	35.9	36.5	36.1	36.6	35.8	36.0
10'	36.4	36.1	36.5	35.8	36.4	35.8	35.9
20'	36.3	35.8	36.2	35.7	36.2	36.0	35.3
30'	36.1	36.2	36.3	35.9	36.4	35.9	/
1 h	36.3	36.2	36.4	36.0	36.3	36.1	/
3 h	36.5	36.1	36.1	35.8	35.9	36.2	/
6 h	36.1	36.3	36.9	36.3	36.0	36.0	/

In addition to the measurements of the above parameters made by the attending medical staff, the enrolled subjects spontaneously reported any other type of symptoms, both during the first 10 hours, when the study was conducted on an outpatient basis, and subsequently, for a total of 48 hours from the start of the study.

Specifically, out of the seven initially enrolled subjects, only six completed the study, as one participant was forced to withdraw early due to the onset of acute symptoms characterized by severe hypotension, nausea, headache, blurred vision, dizziness, and syncope.

Regarding what was observed in the other six enrolled subjects, variable clinical conditions were highlighted, ranging from milder symptoms to more severe clinical conditions where an intense headache occurred along with other milder symptoms.

In particular, xerostomia was observed in 4 out of 6 subjects, conjunctival hyperemia in 3 out of 6 subjects, and a variable severity headache in 3 out of 6 subjects. Speech slowing was observed in 2 out of 6 subjects, and mild motor slowing was observed in 2 out of 6 subjects.

Symptoms were reported by participants mainly in the first phase of observation, with onset between 20 minutes and the first hour after HHC intake. In only one case, the onset of a headache was reported immediately after HHC intake (within 10 minutes).

Clinical symptoms became less pronounced after the first hour, then gradually decreased until almost disappearing after 3 hours from intake.

In the later phase of observation (3-6 hours), 4 out of 6 subjects reported an increase in appetite.

In the extra-ambulatory observation phase, which extended up to the end of the 48 hours from HHC intake, 2 out of 6 subjects reported the onset of diarrhea, and also 2 out of 6 subjects reported fatigue. This symptomatology was temporally located between 10 and 24 hours. No further symptoms were reported thereafter, i.e., between 24 and 48 hours after intake.

Regarding the symptomatology, it can be highlighted that "subject 7," who developed more severe symptoms with nausea, headache, blurred vision, dizziness, and severe hypotension up to syncope, was female and a non-smoker.

“Subject 4”, who developed the most intense symptomatology among the participants who completed the study, was female and a smoker.

“Subject 6”, a female and a smoker, showed intermediate severity symptomatology with a headache more severe than other participants, speech slowing, and mild motor slowing.

“Subject 1”, “Subject 2”, “Subject 3”, and “Subject 5” showed milder symptomatology; of these, only “Subject 5” was a tobacco smoker, and all were male.

Table 20 provides detailed information on the objectively observable and reported effects by the enrolled subjects at different time intervals after HHC intake.

Table 20: Scheme of objectively observable signs and symptoms reported by enrolled subjects at different time intervals after HHC intake.

Clinical effects							
Time	Subj. 1	Subj. 2	Subj. 3	Subj. 4	Subj. 5	Subj. 6	Average
0	/	/	/	/	/	/	/
10'	/	/	/	intense headache, conjunctival hyperemia	/	/	hypotension, nausea, headache, blurred vision, dizziness

20'	xerostomia, conjunctival hyperemia	xerostomia	headache, slowed speech	intense headache, conjunctival hyperemia, slowed speech	xerostomia, conjunctival hyperemia	/	hypotension, syncope (withdrawal from the study)
30'	xerostomia, conjunctival hyperemia	/	headache, slowed speech	intense headache, conjunctival hyperemia, slowed speech, slowed motor function, blurred vision	conjunctival hyperemia	headache, xerostomia	/
1 h	conjunctival hyperemia	/	headache	headache, conjunctival hyperemia, slowed motor function	/	headache, slowed speech, slowed motor function	/
3 h	/	increased appetite	increased appetite	headache, increased appetite	/	/	/
6 h	increased appetite	increased appetite	/	/	/	/	/
10 – 24 h	diarrhea	/	diarrhea	fatigue	/	fatigue	/
24 - 48 h	/	/	/	/	/	/	/

8. DISCUSSION

Until today, the harmful potential of HHC had not been described in humans, both because it has only recently caught the attention of consumers and probably due to the lack of effective analytical methods to detect it in biological matrices. In fact, while several studies have been developed and validated to separate HHC epimers in natural and non-natural sources, few have been conducted on animal models, and only one study on human urine of two subjects has been performed.

HHC represents a more economical and readily available alternative to THC, as its production is relatively simple and can be obtained from natural sources. As previously detailed, HHC can be obtained through a simple hydrogenation reaction of Δ^9 -THC or, with an acid-catalyzed reaction to obtain Δ^9 -THC and Δ^8 -THC from legally marketed CBD and subsequent hydrogenation.

In summary, semi-synthetic HHC represents a legal alternative to illicit THC in many countries by simple Δ^8 -THC or Δ^9 -THC reduction. Furthermore, the total enantioselective synthesis of HHC isomers has recently been achieved through the Diels-Alder reaction.

Due to the lack of in-depth studies on this molecule, many EU countries have decided to ban HHC as its effects would be similar to those of THC. In particular, Austria, Finland, and Estonia were the first European countries to impose bans on the production, sale, and use of HHC, including as a liquid in electronic cigarettes; they were followed by Sweden, Belgium, Denmark, the United Kingdom, and France. Since July 13, 2023, HHC has been included in Table I of narcotic substances (Decree 309/90 of the Ministry of Health), and therefore classified among illicit substances in Italy as well. Currently, HHC is legal in Croatia, Slovenia, Portugal, Spain, Malta, Greece, Cyprus, Ireland, Luxembourg, Moldova, and Romania.

The few studies conducted have confirmed that HHC exhibits typical cannabinoid effects both in vivo and in vitro; however, it seems less potent than its analogue. In particular, based on tests on rhesus monkeys, considered the most suitable and relevant test to assess the psychotropic activity of cannabinoids, it appears that HHC is less potent than Δ^9 -THC. Furthermore, the in vitro affinity for cannabinoid receptors differs for 9S-HHC and 9R-HHC, and various authors indicate that the R epimer has a higher affinity for the CB1 receptor, while the S

epimer has a lower receptor affinity. This suggests that different epimeric mixtures obtained through the semi-synthetic process can induce variable clinical effects.

Currently, the potency, efficacy, and adverse effects of HHC are largely unknown and, therefore, potentially dangerous to health and public safety. In addition, HHC is not commonly investigated in routine toxicological tests, and knowledge of its effects on humans is limited to anecdotal reports brought to the attention of healthcare professionals in cases of intoxication.

Based on these premises, one of the aims of this thesis was to understand the metabolism of HHC through *in silico* prediction and incubation of hepatocytes with subsequent analysis in LC-HRMS/MS. This was followed by the development and validation of an analytical method in ultra-high-performance liquid chromatography coupled with tandem mass spectrometry (UHPLC-MS/MS) for the determination and quantification of HHC in the forms of the two stereoisomers 9R-HHC and 9S-HHC and its main metabolites in biological matrices. This developed and validated method was subsequently applied to real samples taken from seven healthy subjects after consuming cigarettes containing HHC.

The work thus laid the groundwork for the study of HHC pharmacokinetics in humans and the study of clinical effects resulting from its intake.

In the first phase of the study, the metabolism of HHC was assessed through the *in vitro* formation of metabolites after the inoculation of the two epimers of HHC (9S-HHC and 9R-HHC) with a pool of human hepatocytes. The incubates were analyzed by HRMS/MS-MS through a complete data scan. The main metabolites were hydroxy-(9S)-HHC-glucuronide (S3) and 11-hydroxy-(9S)-HHC-glucuronide (S4) for 9S-HHC and dihydroxy-(9R)-HHC-glucuronide (R3) and hydroxy-(9R)-HHC-glucuronide (R7) for 9R-HHC.

The results obtained were compared with three urine samples taken from three male subjects who declared HHC consumption in the previous hours.

In non-hydrolyzed urine, the primary metabolites identified for 9S-HHC were hydroxy-(9S)-HHC-glucuronide (M7); the primary metabolites of (9R)-HHC were dihydroxy-(9R)-HHC-glucuronide (M1) and hydroxy-(9R)-HHC-glucuronide (M10).

In hydrolyzed urine, primary metabolites were dihydroxy-(9S)-HHC and/or dihydroxy-(9R)-HHC (M3, M4) and hydroxy-(9S)-HHC and/or hydroxy-(9R)-HHC (M16).

11-COOH-S-HHC (M19), 11-COOH-R-HHC (M18), 11-OH-S-HHC or 11-OH-R-HHC (M17), and 9- β -OH-HHC (M15) were detected in hydrolyzed urine, but all as minor metabolites.

8-OH-R-HHC and/or 8-OH-R-HHC was/were also found in some of the hydrolyzed urine samples, but the intensity was below the threshold.

Several glucuronides in the hydrolyzed urine samples were only partially hydrolyzed.

It was observed that the metabolites of 9S- and 9R-HHC most detected in vitro were also found in the urine samples of the 3 occasional HHC users, where all the main determined metabolites were glucuronides.

In particular it was possible to identify in both the hydroxy-(9S)-HHC-glucuronide (S4-M7), dihydroxy-(9R)-HHC-glucuronide (R1-M1) and hydroxy-(9R)-HHC-glucuronide (R5-M10).

From this initial phase of the in silico and in vitro study, a first difference in the metabolism of the two epimers of HHC was highlighted, with potential implications on their effects, as well as their detectability and discrimination.

Based on what has been exposed, is it possible to hypothesize a metabolic fate like the one illustrated in figure 25.

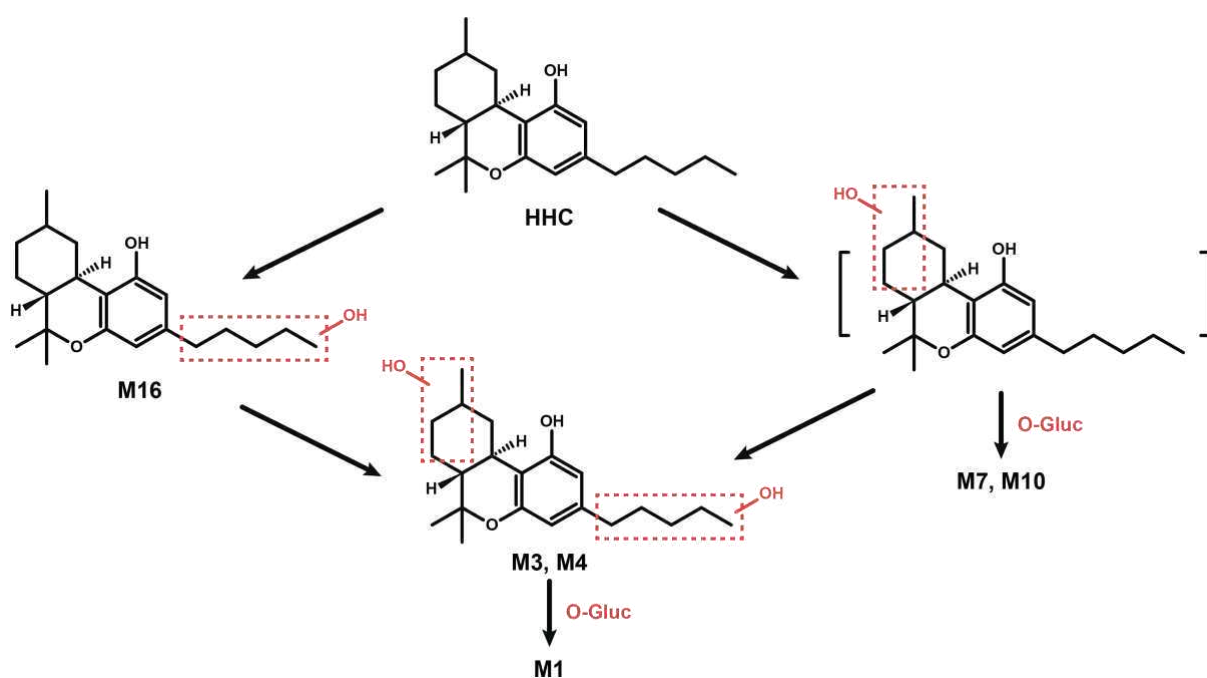


Fig. 25: HHC suggested metabolic fate.

Another evidence emerging in this phase of the study is that the main metabolites of THC were not detected either in vitro or in vivo.

In contrast to the metabolism of Δ^9 -THC, whose main reactions are hydroxylation and subsequent carboxylation at position C11, hydroxylation at the

pentyl chain was also observed. Neither 11-Nor-9S-COOH-HHC nor 11-Nor-9R-COOH-HHC was identified as urinary main metabolite, however the carboxy-metabolites can be regarded as minor metabolites, potentially accumulating after repeated use.

Subsequently, for the first time, an UHPLC-MS/MS method was developed and fully validated for the stereoselective determination and quantification of 9R- and 9S-HHC and some of their metabolites in multiple human biological samples.

The developed method showed good selectivity and specificity; moreover, the simple and rapid sample preparation makes the method suitable for routine analysis. The application of the method to human biological samples (blood, urine, and oral fluid) confirmed that the metabolites of 9S-HHC are hydroxy-(9S)-HHC-glucuronide and 11-hydroxy-(9S)-HHC-glucuronide, and those of 9R-HHC are dihydroxy-(9R)-HHC-glucuronide and hydroxy-(9R)-HHC-glucuronide.

The method was applied to blood, urine, and oral fluid samples to confirm the preliminary results obtained.

For this purpose, an in vivo study was conducted on 7 healthy volunteers who smoked 1 cigarette containing 25 mg of HHC mixture in 500 mg of tobacco and then provided blood, urine, and oral fluid samples.

As previously reported, the peak plasma concentration was reached approximately 20 minutes after intake, and the average maximum concentration was 30.02 ng/mL for 9R-HHC and 13.03 ng/mL for 9S-HHC. Regarding the analysis of urine samples, the maximum concentration was 8.88 ng/mL for 9R-HHC (with a maximum peak at 6 hours after HHC intake) and 14.7 ng/mL for 9S-HHC (with a maximum peak at 3 hours after HHC intake). The concentrations detected in oral fluids were at least 10 times higher than those found in other biological matrices (129.35 ng/mL for 9R-HHC and 99.25 ng/mL for 9S-HHC with peaks at 20 and 10 minutes, respectively).

For the metabolites, only 11-NOR-9R-COOH-HHC was detected and quantified in the blood samples of two subjects; the plasma peak was at 30 minutes and 1 hour, respectively. The same metabolite represented the most abundant in urine, although isomers 11-NOR-9S-COOH-HHC, 11-OH-9R-HHC, and 9 α -OH-HHC were also detected. 11-NOR-9R-COOH-HHC, the most produced metabolite,

had a maximum average urinary concentration of 21.53 ng/mL 6 hours after HHC intake. As hypothesized, and similarly to the original substance, the 9R-epimer of this metabolite was consistently detected at higher concentrations than the 9S- in all analyzed urine samples.

In all 168 biological samples analyzed, the 9R-epimer was always detected at higher concentrations than the 9S-HHC isomer, suggesting a marked stereoselectivity in the metabolism and pharmacokinetics of this cannabinoid.

These data, together with what was previously illustrated, confirm the thesis that there is strong stereoselectivity in the metabolism and pharmacokinetics of HHC.

It is also important to note that the present study is limited to the analysis of biological samples from HHC smokers. To better understand the metabolic profile, further studies are needed to consider other routes of administration, primarily oral ingestion. It is possible to hypothesize that the administration route might impact metabolism, both due to varying absorption rates and first-pass effects.

Understanding the pharmacokinetics and effects of HHC is a crucial challenge not only concerning the social and health issues related to recreational substance use but also to better comprehend its effects and assess potential therapeutic effects.

The *in vivo* study also aimed to evaluate the clinical symptoms that occurred after the intake of HHC in enrolled subjects. To this end, the vital parameters of the study participants (blood pressure, heart rate, saturation, and body temperature) were measured, and subjective symptoms were documented, both in the outpatient observation phase (first 10 hours) and subsequently, up to 48 hours after HHC intake.

Regarding the detection of these vital parameters, with respect to blood pressure, a contained increase in values (approximately 10 mmHg) was appreciated in most subjects. Conversely, in the two subjects who developed hypotension, this was related to more significant side effects. In detail, in one case, the subject complained of headache, blurred vision, and dizziness and, simultaneously with the decrease in blood pressure values, experienced a syncope episode that led to the abandonment of the study; in the second, symptoms characterized by headache, blurred vision, conjunctival hyperemia, slowed speech, and slowed motor activity

developed, symptoms that, although significant, were self-limiting. In both reported cases, the symptoms were more acute concurrently with the peak blood concentration of HHC, i.e., at 20 and 30 minutes after intake.

As for the other measured parameters, a slight increase in heart rate was observed in all subjects in the study. This was more significant in the 2 cases where a significant vasopressor reaction with hypotension and concomitant tachycardia was observed, while in other cases, the increase in frequency was moderate. Regarding the other recorded parameters, namely oxygen saturation and body temperature, no significant variations were observed during observation.

In addition to the aforementioned measurements made by the attending medical staff, the enrolled subjects spontaneously reported any other type of developed symptoms.

Of the 7 subjects initially enrolled, only 6 completed the study, as one participant was forced to leave the project prematurely following the development of acute symptoms.

In other enrolled subjects, variable clinical conditions were appreciated, from milder symptomatology to conditions of greater clinical severity where intense

headache occurred along with other milder symptoms. The signs and symptoms mainly observed were xerostomia, conjunctival hyperemia, and variable severity headache, followed by slowed speech and motor slowing. The more acute symptoms were reported by participants in the initial observation phase, with onset between 20 minutes and the first hour after HHC intake, i.e., concurrently with the concentration peaks of HHC. The clinical picture faded after the first hour, then almost completely disappeared after 3 hours following intake.

In the later phase of outpatient observation (3-6 hours), most enrolled subjects reported an increase in appetite. In the early stage of outpatient observation (between 10 and 24 hours after intake), one-third of the subjects reported fatigue, and an equal number reported the onset of diarrhea. No further symptoms were revealed over time.

The subject who dropped out of the study due to the development of hypotension with syncope and the two subjects who presented more severe symptoms were female, while those who showed milder symptoms were male. A larger number of subjects would be necessary to establish whether this observation

is due to chance or to a different distribution pattern among the men and women involved in the study.

From the obtained data, there was no evidence of a correlation between smoking habits and the severity of clinical symptoms developed.

From these data, although acquired on a small sample of subjects, it is possible to affirm that HHC induces rather variable clinical effects. The symptomatology recorded in enrolled subjects had characteristics overlapping with the well-known THC, with a wide variability of interindividual manifestations, ranging from mild clinical effects to severe adverse reactions. This reflects a different activation of the ECS in individual subjects and therefore significant subjective variability, in line with what is observed in cannabinoid toxicity.

In addition, as confirmed in this study, HHC shows strong stereoselectivity in metabolism and pharmacokinetics. This allows confirming what was already hypothesized in the relevant literature, namely that the 9R-HHC isomer is precisely the one mainly responsible for the cannabinomimetic activity and therefore the reported clinical effects.

In our study, 9R-HHC was systematically detected at higher concentrations than its epimer and had higher concentrations in all biological matrices of subjects who presented more severe symptoms than those who developed milder symptoms.

These data demonstrate a variable potency of HHC, different from what was initially hypothesized at the beginning of its diffusion when it was marketed as “light cannabis”.

Based on the obtained data, some considerations regarding HHC-based products available on the market and the possible consequences secondary to their use are necessary. As already described, commercially available HHC products do not specify the quantities of the two isomers contained in different mixtures. It is therefore obvious that products with a higher amount of 9R-HHC will determine more severe clinical effects with possible acute toxicity. It follows that even regular HHC users can develop clinical symptoms of varying severity with different assumptions, attributable to an inconsistent concentration of the two epimers in the various purchased products.

9. CONCLUSIONS

The monitoring of HHC represents a crucial challenge for forensic toxicologists. In view of its widespread use, the evidence reported in the relevant literature, and based on the data acquired from this work, it can be stated that the consumption of HHC and other synthetic cannabinoids may pose risks to individual health and public health.

Therefore, it is necessary to acquire further information regarding usage clusters, the illicit market, as well as to investigate in detail the metabolic pathways, acute and chronic toxicity, and the potential interaction with other substances of abuse. The availability of HHC and other cannabinoids on the web poses a serious health problem because the psychoactive substances made freely available expose consumers to a high risk of acute intoxication. Furthermore, in case of intoxication, the lack of detailed information regarding the active ingredients contained in products purchased online, and in the specific case the concentrations of the two epimers of HHC, makes it difficult for healthcare

professionals to formulate an accurate diagnosis and, therefore, provide immediate assistance to the patient.

In this regard, it is crucial, both from a forensic and clinical perspective, to introduce methods for the determination and quantification of HHC and its metabolites into clinical practice and in screenings conducted in cases of acute intoxication. It is therefore essential to maintain a high level of attention on HHC despite the recent change in its status as an illicit substance. It is also necessary to continue careful monitoring of new cannabinoids in order to intercept them promptly and avoid the possible harmful consequences of their use on both individual and public health.

10. BIBLIOGRAPHY

1. Hanus LO, Meyer SM, Munoz E, Taglialatela-Scafati O, Appendino G. *Phytocannabinoids: a unified critical inventory*. Nat Prod Rep **2016**; 33:1357–1392.
2. Brunetti P, Pichini S, Pacifici R, Busardò FP, Del Rio A. *Herbal Preparations of Medical Cannabis: A Vademecum for Prescribing Doctors*. Medicina (Kaunas). **2020**;56:237.
3. Verga M. *Cannabis: La "Droga" e il "Farmaco". Una rassegna della letteratura dal 1970 ad oggi*. Centro Interuniversitario per le ricerche sulla Sociologia del Diritto e delle Istituzioni Giuridiche - C.I.R.S.D.I.G. **2007**.
4. Mead A. *Legal and Regulatory Issues Governing Cannabis and Cannabis-Derived Products in the United States*. Front Plant Sci. **2019**; 14;10:697.
5. *World Drug Report 2022*. United Nations publication, Sales No. 22.XI.8.
6. Brenneisen, R. *Chemistry and Analysis of Phytocannabinoids and Other Cannabis Constituents*. In *Marijuana and the Cannabinoids*; ElSohly, M.A., Ed.; Forensic Science And Medicine; Humana Press: Totowa, NJ, **2007**; pp. 17–49.
7. Sirikantaramas, S.; Taura, F. *Cannabinoids: Biosynthesis and Biotechnological Applications*. In *Cannabis sativa L. - Botany and Biotechnology*; Chandra, S., Lata, H., ElSohly, M.A., Eds.; Springer International Publishing: Cham, **2017**; pp. 183–206.
8. Bonini, S.A.; Premoli, M.; Tambaro, S.; Kumar, A.; Maccarinelli, G.; Memo, M.; Mastinu, A. *Cannabis sativa: A comprehensive ethnopharmacological review of a medicinal plant with a long history*. J. Ethnopharmacol. **2018**, 227, 300–315.
9. Di Forti M, et al. *The contribution of cannabis use to variation in the incidence of psychotic disorder across Europe (EU-GEI): a multicentre case-control study*. Lancet Psychiatry. **2019**;6:427-436.

10. Pertwee, R.G. *The diverse CB1 and CB2 receptor pharmacology of three plant cannabinoids: Δ 9-tetrahydrocannabinol, cannabidiol and Δ 9-tetrahydrocannabivarin*. Br. J. Pharmacol. **2008**, 153, 199–215.
11. Izzo, A.A.; Borrelli, F.; Capasso, R.; Marzo, V.D.; Mechoulam, R. *Non-psychotropic plant cannabinoids: new therapeutic opportunities from an ancient herb*. Trends Pharmacol. Sci. **2009**, 30, 515–527.
12. Casajuana Köguel, C.; López-Pelayo, H.; Balcells-Olivero, M.M.; Colom, J.; Gual, A. *Constituyentes psicoactivos del Cannabis y sus implicaciones clínicas: una revisión sistemática*. Adicciones **2018**; 30:140–151.
13. White CM. *A Review of Human Studies Assessing Cannabidiol's (CBD) Therapeutic Actions and Potential*. J Clin Pharmacol. **2019**;59:923-934.
14. Laun, A.S.; Shrader, S.H.; Brown, K.J.; Song, Z.-H. *GPR3, GPR6, and GPR12 as novel molecular targets: their biological functions and interaction with cannabidiol*. Acta Pharmacol. Sin. **2019**; 40:300–308.
15. Ujváry I. *Hexahydrocannabinol and closely related semi-synthetic cannabinoids: A comprehensive review*. Drug Test Anal. **2023**. Epub ahead of print.
16. European Monitoring Centre for Drugs and Drug Addiction, Lisbon, **2022**.
17. Castaneto MS, Gorelick DA, Desrosiers NA, Hartman RL, Pirard S, Huestis MA. *Synthetic cannabinoids: epidemiology, pharmacodynamics, and clinical implications*. Drug Alcohol Depend. **2014**;1;144:12-41.
18. Fattore L, Fratta W. *Beyond THC: The New Generation of Cannabinoid Designer Drugs*. Front Behav Neurosci. **2011**;21;5:60.
19. UNODC. *Early warning advisory (EWA) on new psychoactive substances (NPS)*. (United Nations Office on Drugs and Crime **2017**).

20. Musselman ME, Hampton JP. *"Not for human consumption": a review of emerging designer drugs*. *Pharmacotherapy*. **2014**;34:745-57.
21. Banister SD, Stuart J, Kevin RC, Edington A, Longworth M, Wilkinson SM, Beinat C, Buchanan AS, Hibbs DE, Glass M, Connor M, McGregor IS, Kassiou M. *Effects of bioisosteric fluorine in synthetic cannabinoid designer drugs JWH-018, AM-2201, UR-144, XLR-11, PB-22, 5F-PB-22, APICA, and STS-135*. *ACS Chem Neurosci*. **2015**;19;6:1445-58.
22. Brunt TM, Bossong MG. *The neuropharmacology of cannabinoid receptor ligands in central signaling pathways*. *Eur J Neurosci*. **2022**;55:909-921.
23. Lu HC, Mackie K. *Review of the Endocannabinoid System*. *Biol Psychiatry Cogn Neurosci Neuroimaging*. **2021**;6:607-615.
24. Di Marzo, V., Piscitelli, F. *The Endocannabinoid System and its Modulation by Phytocannabinoids*. *Neurotherapeutics* 2015;12:692–698.
25. Van der Stelt M, Di Marzo V. *Cannabinoid receptors and their role in neuroprotection*. *Neuromolecular Med*. **2005**;7:37-50.
26. Ye L, Cao Z, Wang W, Zhou N. *New Insights in Cannabinoid Receptor Structure and Signaling*. *Curr Mol Pharmacol*. **2019**;12:239-248.
27. Amin MR, Ali DW. *Pharmacology of Medical Cannabis*. *Adv Exp Med Biol*. **2019**;1162:151-165.
28. Devane WA, Dysarz FA 3rd, Johnson MR, Melvin LS, Howlett AC. *Determination and characterization of a cannabinoid receptor in rat brain*. *Mol Pharmacol*. **1988**;34:605-13.
29. Matsuda LA, Lolait SJ, Brownstein MJ, Young AC, Bonner TI. *Structure of a cannabinoid receptor and functional expression of the cloned cDNA*. *Nature*. **1990**;9;346:561-4.
30. Gérard CM, Mollereau C, Vassart G, Parmentier M. *Molecular cloning of a human cannabinoid receptor which is also expressed in testis*. *Biochem J*. **1991**;1;279.

31. Turu G, Hunyady L. *Signal transduction of the CB1 cannabinoid receptor*. J Mol Endocrinol. **2010**;44:75-85.
32. Biegon A, Kerman IA. *Autoradiographic study of pre- and postnatal distribution of cannabinoid receptors in human brain*. Neuroimage. **2001**;14:1463-8.
33. Mailleux P, Vanderhaeghen JJ. *Localization of cannabinoid receptor in the human developing and adult basal ganglia. Higher levels in the striatonigral neurons*. Neurosci Lett. **1992** 14;148:173-6.
34. Pettit DA, Harrison MP, Olson JM, Spencer RF, Cabral GA. *Immunohistochemical localization of the neural cannabinoid receptor in rat brain*. J Neurosci Res. **1998**;1;51:391-402.
35. Kano M, Ohno-Shosaku T, Hashimotodani Y, Uchigashima M, Watanabe M. *Endocannabinoid-mediated control of synaptic transmission*. Physiol Rev. **2009**;89:309-80.
36. Alger BE. *Endocannabinoids at the synapse a decade after the dies mirabilis (29 March 2001): what we still do not know*. J Physiol. **2012**;15;590:2203-12.
37. Iannotti FA et al. *The endocannabinoid 2-AG controls skeletal muscle cell differentiation via CB1 receptor-dependent inhibition of Kv7 channels*. Proc Natl Acad Sci U S A. **2014**;17;111:E2472-81.
38. Zou S, Kumar U. *Cannabinoid Receptors and the Endocannabinoid System: Signaling and Function in the Central Nervous System*. Int J Mol Sci. **2018**;13;19:833.
39. Kill JB, Oliveira IF, Tose LV, Costa HB, Kuster RM, Machado LF, Correia RM, Rodrigues RRT, Vasconcellos GA, Vaz BG, Romão W. *Chemical characterization of synthetic cannabinoids by electrospray ionization FT-ICR mass spectrometry*. Forensic Sci Int. **2016**;266:474-487.
40. Hohmann AG, Briley EM, Herkenham M. *Pre- and postsynaptic distribution of cannabinoid and mu opioid receptors in rat spinal cord*. Brain Res. **1999**;20;822:17-25.

41. Munro S, Thomas KL, Abu-Shaar M. *Molecular characterization of a peripheral receptor for cannabinoids*. Nature. **1993**;2;365:61-5.
42. Lutz B. *Neurobiology of cannabinoid receptor signaling*. Dialogues Clin Neurosci. **2020**;22:207-222.
43. Staiano RI, Loffredo S, Borriello F, Iannotti FA, Piscitelli F, Orlando P, Secondo A, Granata F, Lepore MT, Fiorelli A, Varricchi G, Santini M, Triggiani M, Di Marzo V, Marone G. *Human lung-resident macrophages express CB1 and CB2 receptors whose activation inhibits the release of angiogenic and lymphangiogenic factors*. J Leukoc Biol. **2016**;99:531-40.
44. Annuzzi G, Piscitelli F, Di Marino L, Patti L, Giacco R, Costabile G, Bozzetto L, Riccardi G, Verde R, Petrosino S, Rivellese AA, Di Marzo V. *Differential alterations of the concentrations of endocannabinoids and related lipids in the subcutaneous adipose tissue of obese diabetic patients*. Lipids Health Dis. **2010**;28;9:43.
45. Galli JA, Sawaya RA, FriedenberG FK. *Cannabinoid hyperemesis syndrome*. Curr Drug Abuse Rev. **2011**;4:241-9.
46. Stella N., *Cannabinoid and cannabinoid-like receptors in microglia, astrocytes, and astrocytomas*. Glia. **2010**;58:1017-1030.
47. Xi ZX, Peng XQ, Li X, Song R, Zhang HY, Liu QR, Yang HJ, Bi GH, Li J, Gardner EL. *Brain cannabinoid CB₂ receptors modulate cocaine's actions in mice*. Nat Neurosci. **2011**;24;14:1160-6.
48. Malfitano, Anna Maria et al., *What we know and do not know about the cannabinoid receptor 2 (CB2)*. Seminars in immunology **2014**;26: 369-79.
49. Demuth DG, Molleman A. *Cannabinoid signalling*. Life Sci. **2006**;2;78:549-63.
50. Krishna Kumar K, Shalev-Benami M, Robertson MJ, Hu H, Banister SD, Hollingsworth SA, Latorraca NR, Kato HE, Hilger D, Maeda S, Weis WI, Farrens DL, Dror RO, Malhotra SV,

Kobilka BK, Skiniotis G. *Structure of a Signaling Cannabinoid Receptor 1-G Protein Complex*. Cell. **2019**;24;176:448-458.

51. Howlett, Allyn C, and Mary E Abood. *CBI and CB2 Receptor Pharmacology*. Advances in pharmacology (San Diego, Calif.) **2017**;80:169-206.

52. Lauckner JE, Jensen JB, Chen HY, Lu HC, Hille B, Mackie K. *GPR55 is a cannabinoid receptor that increases intracellular calcium and inhibits M current*. Proc Natl Acad Sci U S A. **2008**;19;105:2699-704.

53. Iannotti FA, Hill CL, Leo A, Alhusaini A, Soubrane C, Mazzarella E, Russo E, Whalley BJ, Di Marzo V, Stephens GJ. *Nonpsychotropic plant cannabinoids, cannabidivarin (CBDV) and cannabidiol (CBD), activate and desensitize transient receptor potential vanilloid 1 (TRPV1) channels in vitro: potential for the treatment of neuronal hyperexcitability*. ACS Chem Neurosci. **2014**;19;5:1131-41.

54. de Almeida DL, Devi LA. *Diversity of molecular targets and signaling pathways for CBD*. Pharmacol Res Perspect. **2020**;8:e00682.

55. Devane WA, Hanus L, Breuer A, Pertwee RG, Stevenson LA, Griffin G, Gibson D, Mandelbaum A, Etinger A, Mechoulam R. *Isolation and structure of a brain constituent that binds to the cannabinoid receptor*. Science. **1992**;18;258:1946-9.

56. Mechoulam R, Ben-Shabat S, Hanus L, Ligumsky M, Kaminski NE, Schatz AR, Gopher A, Almog S, Martin BR, Compton DR, et al. *Identification of an endogenous 2-monoglyceride, present in canine gut, that binds to cannabinoid receptors*. Biochem Pharmacol. **1995**;29;50:83-90.

57. Hanus L, Abu-Lafi S, Fride E, Breuer A, Vogel Z, Shalev DE, Kustanovich I, Mechoulam R. *2-arachidonyl glyceryl ether, an endogenous agonist of the cannabinoid CBI receptor*. Proc Natl Acad Sci U S A. **2001**;27;98:3662-5.

58. Lu HC, Mackie K. An Introduction to the Endogenous Cannabinoid System. *Biol Psychiatry*. **2016**;1;79:516-25.
59. Fezza F, Bari M, Florio R, Talamonti E, Feole M, Maccarrone M. *Endocannabinoids, related compounds and their metabolic routes*. *Molecules*. **2014**;19:17078-17106.
60. Verbanck P. *Short-term and long-term effects of cannabis use*. *Rev Med Brux*. **2018**;39:246-249.
61. Cohen K, Weizman A, Weinstein A. *Positive and Negative Effects of Cannabis and Cannabinoids on Health*. *Clin Pharmacol Ther*. **2019**;105:1139-1147.
62. Ashton CH. *Pharmacology and effects of cannabis: a brief review*. *Br J Psychiatry*. **2001**;178:101-6.
63. Connor JP, Stjepanović D, Le Foll B, Hoch E, Budney AJ, Hall WD. *Cannabis use and cannabis use disorder*. *Nat Rev Dis Primers*. **2021**;25;7:16.
64. Karila L, Roux P, Rolland B, Benyamina A, Reynaud M, Aubin HJ, Lançon C. *Acute and long-term effects of cannabis use: a review*. *Curr Pharm Des*. **2014**;20:4112-8.
65. Chayasirisobhon S. *Mechanisms of Action and Pharmacokinetics of Cannabis*. *Perm J*. **2020**;25:1-3.
66. Grotenhermen F. *Pharmacokinetics and pharmacodynamics of cannabinoids*. *Clin Pharmacokinet*. **2003**;42:327–360.
67. Wong KU, Baum CR. *Acute Cannabis Toxicity*. *Pediatr Emerg Care*. **2019**;35:799-804.
68. Jiang HE, Li X, Zhao YX, Ferguson DK, Hueber F, Bera S, Wang YF, Zhao LC, Liu CJ, Li CS. *A new insight into Cannabis sativa (Cannabaceae) utilization from 2500-year-old Yanghai Tombs, Xinjiang, China*. *J Ethnopharmacol*. **2006**;6;108:414-22.
69. Schifano, F., Orsolini, L., Papanti, D. & Corkery, J. *NPS: Medical Consequences Associated with Their Intake*. *Curr. Top. Behav. Neurosci*. **2017**;32:351-380.

70. Kelly BF, Nappe TM. *Cannabinoid Toxicity*. **2023**. In: StatPearls [Internet]. Treasure Island (FL): StatPearls Publishing.
71. Coronado-Álvarez A, Romero-Cordero K, Macías-Triana L, Tatum-Kuri A, Vera-Barrón A, Budde H, Machado S, Yamamoto T, Imperatori C, Murillo-Rodríguez E. *The synthetic CBI cannabinoid receptor selective agonists: Putative medical uses and their legalization*. *Prog Neuropsychopharmacol Biol Psychiatry*. **2021**;30;110:110301.
72. Serpelloni G, Macchia T, Locatelli C, Rimondo C, Seri C. *Nuove Sostanze Psicoattive (NSP): schede tecniche relative alle molecole registrate dal Sistema Nazionale di Allerta Precoce*.**2013**.
73. Hermanns-Clausen M, Kneisel S, Szabo B, Auwärter V. *Acute toxicity due to the confirmed consumption of synthetic cannabinoids: clinical and laboratory findings*. *Addiction*. **2013**;108:534-44.
74. Jinwala FN, Gupta M. *Synthetic cannabis and respiratory depression*. *J Child Adolesc Psychopharmacol*. **2012**;22:459-62.
75. Skipina TM, Upadhyay B, Soliman EZ. *Cannabis Use and Electrocardiographic Myocardial Injury*. *Am J Cardiol*. **2021**;15;151:100-104.
76. Bhanushali GK, Jain G, Fatima H, Leisch LJ, Thornley-Brown D. *AKI associated with synthetic cannabinoids: a case series*. *Clin J Am Soc Nephrol*. **2013**;8:523-6.
77. Perisetti A, Gajendran M, Dasari CS, Bansal P, Aziz M, Inamdar S, Tharian B, Goyal H. *Cannabis hyperemesis syndrome: an update on the pathophysiology and management*. *Ann Gastroenterol*. **2020**;33:571-578.
78. Trappey BE, Olson APJ. *Running Out of Options: Rhabdomyolysis Associated with Cannabis Hyperemesis Syndrome*. *J Gen Intern Med*. **2017**;32:1407-1409.

79. Swetlik C, Migdady I, Hasan LZ, Buletko AB, Price C, Cho SM. *Cannabis Use and Stroke: Does a Risk Exist?* J Addict Med. **2022**;01;16:208-215.
80. Brunetti P, Lo Faro AF, Pirani F, Berretta P, Pacifici R, Pichini S, Busardò FP. *Pharmacology and legal status of cannabidiol*. Ann Ist Super Sanita. **2020**;56:285-291.
81. Adams R. US 2419937 - *Marihuana Active Compounds*. **1947**.
82. Adams, R., Pease, D., Cain, C. & Clark, J. *Structure of cannabidiol. VI. Isomerization of cannabidiol to tetrahydrocannabinol, a physiologically active product. Conversion of cannabidiol to cannabinol*. J. Am. Chem. Soc. 62, 2402–2405. **1940**.
83. TODD AR. *Hashish [Hashish]*. *Experientia*. **1946**;15;2:55-60.
84. U.S. Public Law. *Agriculture improvement act of 2018*. Public Law 115–334. **2018**. 115th Congress.
85. Geci M, Scialdone M, Tishler J. *The dark side of cannabidiol: the unanticipated social and clinical implications of synthetic $\Delta 8$ -THC*. Cannabis Cannabinoid Res. **2023**;8:270-28222–25.
86. Erickson BE. *Delta-8-THC craze concerns chemists*. Chem Eng News. **2021**;99:24-28.
87. European Monitoring Centre for Drugs and Drug Addiction. Technical Report. *Hexahydrocannabinol (HHC) and Related Substances 2023*. Publications Office of the European Union; **2023**.
88. Basas-Jaumandreu J, de Las Heras FX, *GC-MS Metabolite Profile and Identification of Unusual Homologous Cannabinoids in High Potency Cannabis sativa*. Planta Medica. 2020;86;5:338–347.
89. Harvey DJ, Brown NK, *In vitro metabolism of the equatorial C11-methyl isomer of hexahydrocannabinol in several mammalian species*. Drug Metabolism and Disposition. **1991**;19;3:714–716.

90. Graziano S, Vari MR, Pichini S, Busardo FP, Cassano T, Di Trana A. *Hexahydrocannabinol Pharmacology, Toxicology, and Analysis: The First Evidence for a Recent New Psychoactive Substance*. *Curr Neuropharmacol*. **2023**;21:2424-2430.
91. Archer, R. A., Boyd, D. B., Demarco, P. V., Tyminski, I. J. & Allinger, N. L. *Structural studies of cannabinoids. Theoretical and proton magnetic resonance analysis*. *J. Am. Chem. Soc.* **1992**; 5200- 5206.
92. Reggio PH, Greer KV, Cox SM. *The importance of the orientation of the C9 substituent to cannabinoid activity*. *J Med Chem*. **1989**;32:1630-1635.
93. Casati S, Rota P, Bergamaschi RF, Palmisano E, La Rocca P, Ravelli A, Angeli I, Minoli M, Roda G, Orioli M. *Hexahydrocannabinol on the Light Cannabis Market: The Latest "New" Entry*. *Cannabis Cannabinoid Res*. **2022**.
94. Edery H, Grunfeld Y, Ben-Zvi Z, Mechoulam R. *Structural requirements for cannabinoid activity*. *Ann N Y Acad Sci*. **1971**;191:40-53.
95. Russo F, Vandelli MA, Biagini G, et al. *The semisynthetic cannabinoid hexahydrocannabinol (HHC)*. Preprint. Research Square; **2023**.
96. Cannabis Chemistry Subdivision of the American Chemical Society. **2021**.
97. Perez-Reyes M, Lipton MA, Timmons MC, Wall ME, Brine DR, Davis KH. *Pharmacology of orally administered 9 -tetrahydrocannabinol*. *Clin Pharmacol Ther*. **1973**;14:48-55.
98. Collins A, Ramirez G, Tesfatsion T, Ray KP, Caudill S, Cruces W. *Synthesis and characterization of the diastereomers of HHC and H4CBD*. *Nat Prod Commun*. **2023**;18.
99. Harvey DJ, Brown NK. *A method based on catalytic hydrogenation for the identification of monohydroxy metabolites of isomeric tetrahydrocannabinols*. *Rapid Commun Mass Spectrom*. **1990**;4:67-68.

100. Nahler G, Grotenhermen F, Zuardi AW, Crippa JAS. *A Conversion of Oral Cannabidiol to Delta9-Tetrahydrocannabinol Seems Not to Occur in Humans*. *Cannabis Cannabinoid Res.* **2017**;1;2:81-86.
101. Nasrallah DJ, Garg NK. *Studies Pertaining to the Emerging Cannabinoid Hexahydrocannabinol (HHC)*. *ACS Chem Biol.* **2023**;15;18:2023-2029.
102. K.M. Yang, Organization of Scientific Area Committees (OSAC) for Forensic Science Standard Practices for Method Development, <https://www.nist.gov/osac>.
103. J. Mandel, *The statistical analysis of experimental data*, *Biom. J.* 10;231-279.
104. B.K. Matuszewski, M.L. Constanzer, C.M. Chavez-Eng, *Strategies for the assessment of matrix effect in quantitative bioanalytical methods based on HPLC-MS/MS*, *Anal. Chem.* **2003**;75:3019–3030.
105. Maurya, V., Appayee, C. *Enantioselective total synthesis of potent 9 β -11-hydroxyhexahydrocannabinol*. *J. Org. Chem.*, **2020**;85:1291-1297.